LA-3229-MS Supplement

C.3

LOS ALAMOS SCIENTIFIC LABORATORY
of the
University of California

LOS ALAMOS • NEW MEXICO

Proceedings of an Advanced Nuclear Propulsion Symposium

UNITED STATES
ATOMIC ENERGY COMMISSION
CONTRACT W-7405-ENG. 36

AEC RESEARCH AND DEVELOPMENT REPORT

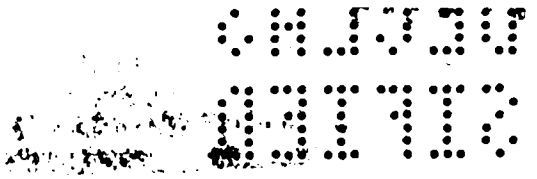

All LA...MS reports are informal documents, usually prepared for a special purpose and primarily prepared for use within the Laboratory rather than for general distribution. This report has not been edited, reviewed, or verified for accuracy. All LA...MS reports express the views of the authors as of the time they were written and do not necessarily reflect the opinions of the Los Alamos Scientific Laboratory or the final opinion of the authors on the subject.

Printed in USA. Charge $1.65. Available from the U. S. Atomic Energy Commission, Technical Information Service Extension, P. O. Box 1001, Oak Ridge, Tennessee. Please direct to the same address inquiries covering the procurement of other classified AEC reports.

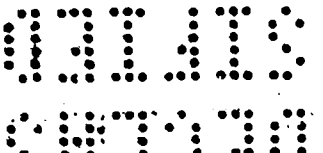

[redacted] Supplement
C-93a, ADVANCED CONCEPTS
FOR FUTURE APPLICATION -
REACTOR EXPERIMENTS
M-3679 (47th Ed.)

UNCLASSIFIED

LOS ALAMOS SCIENTIFIC LABORATORY
of the
University of California
LOS ALAMOS • NEW MEXICO

Report written: January 1965
Report distributed: February 13, 1967

Proceedings of an Advanced Nuclear Propulsion Symposium

Compiled by

Ralph S. Cooper

UNITED STATES
ATOMIC ENERGY COMMISSION
CONTRACT W-7405-ENG. 36

[redacted]

[redacted]

UNCLASSIFIED

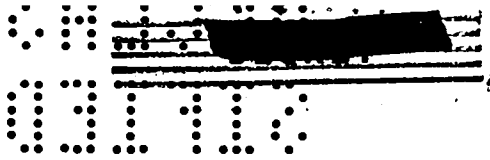

LA-3229-MS Supplement
C-93a, ADVANCED CONCEPTS FOR
FUTURE APPLICATION - REACTOR EXPERIMENTS
M-3679 (47th Ed.)

Los Alamos Report Library	1-30	Lockheed-Georgia Company	86
AEC Patent Office	31	Martin Company	87
Aerojet-General Corporation (NASA)	32-33	Mound Laboratory	88
Aerojet-General Corporation, Sacramento	34	NASA Goddard Space Flight Center	89-90
Aerojet-General Nucleonics (NASA)	35	NASA Langley Research Center	91
Aeronautical Systems Division	36-37	NASA Lewis Research Center	92-98
Aerospace Corporation	38	NASA Manned Spacecraft Center	99
Air Force Headquarters	39	NASA Marshall Space Flight Center	100
Air Force Rocket Propulsion Laboratory	40	National Aeronautics and Space Administration, Washington	101-102
Air Force Technical Applications Center	41	National Reactor Testing Station (INC)	103-104
Air Force Weapons Laboratory	42-44	Naval Air Systems Command	105
Albuquerque Operations Office	45	Naval Ordnance Laboratory	106
Allison Division-GMC	46	Naval Ordnance Systems Command	107-108
Argonne National Laboratory	47	Naval Radiological Defense Laboratory	109
Army Ballistic Research Laboratories	48	Naval Ship Systems Command Headquarters	110-111
Army Chief of Research and Development	49	Navy Marine Engineering Laboratory	112
Army Harry Diamond Laboratories	50	New York Operations Office	113
Army Materials Research Agency	51	Oak Ridge Operations Office	114
Army Reactors Field Group	52	Office of the Chief of Naval Operations	115
Aro, Inc.	53	Pratt and Whitney Aircraft Division (NASA)	116
Atomic Energy Commission, Washington	54-57	Rand Corporation	117
Atomics International	58	Republic Aviation Division	118
Battelle Memorial Institute	59	Sandia Corporation	119-121
Battelle-Northwest	60-65	Tracerlab, Richmond	122
Brookhaven National Laboratory	66	TRW Systems	123
California Patent Group	67	Union Carbide Corporation (ORNL)	124-133
Canoga Park Area Office	68	University of California, Livermore	134-135
Chicago Patent Group	69	Westinghouse Bettis Atomic Power Laboratory	136-138
Cincinnati Area Office	70	Westinghouse Electric Corporation, Lima	139
Director of Defense Research and Engineering	71	Westinghouse Electric Corporation, (NASA)	140
Du Pont Company, Aiken	72	Westinghouse Electric Corporation, (WAL)	141
General Atomic Division	73	Division of Technical Information Extension	142-151
General Dynamics/Fort Worth	74	Radio Corporation of America, Cranbury (AL)	152
General Electric Company, Cincinnati	75-78		
General Electric Company (FPD)	79		
General Electric Company (MSVD)	80		
General Electric Company, San Jose	81		
Jet Propulsion Laboratory	82-83		
Johns Hopkins University (APL)	84		
Knolls Atomic Power Laboratory	85		

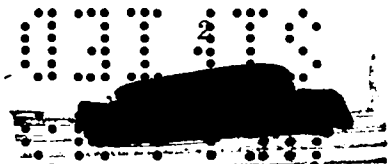

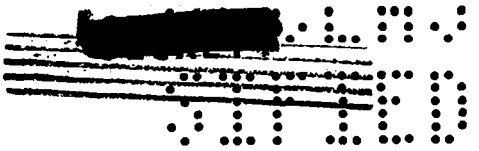

FOREWORD

In April 1964, a small symposium was held at Los Alamos on the subject of advanced nuclear propulsion, by which was meant those concepts beyond the solid core heat exchanger using nuclear energy to produce a high thrust propulsion system. The attendance was limited, but an attempt was made to have at least representatives of all groups active in the field. No formal papers were required and much of the time was spent in discussion, but it was felt that a record of the proceedings would be useful. Transcriptions were made from tape recordings through the courtesy of W. E. Matheson and D. E. Knapp of the Douglas Aircraft Company who also handled the work of obtaining edited copies from the authors. Editing was generally kept to a minimum, so these proceedings retain the informal character of the meeting. Some of the material reported was work in progress and therefore preliminary, and due caution should be exercised in using or quoting results contained herein.

The bulk of the material presented was unclassified (as determined by the organizations making the presentation) and is included in the original document. This supplement includes the classified material that could be obtained. Together they make a reasonably complete but brief survey of the field as of April 1964. Although the primary purpose of the meeting was an exchange of information among a few workers in the field, it is hoped that the proceedings will be useful to others who were unable to attend.

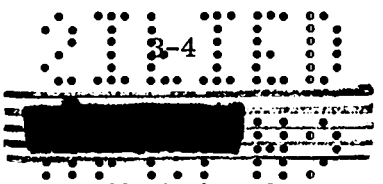

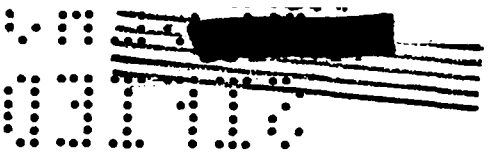

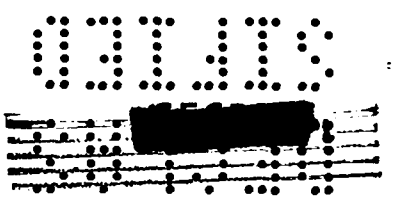

TABLE OF CONTENTS

UNCLASSIFIED

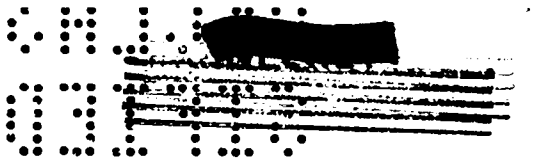

UNCLASSIFIED

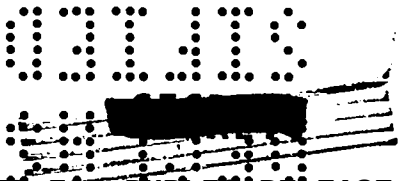

SEPARATION

Major M. Keller
Aerospace Research Laboratories
Office of Aerospace Research
Dayton, Ohio

A copy of this presentation is not available as the edited transcript was not returned by the author.

VORTEX-STABILIZED GASEOUS NUCLEAR ROCKET

George H. McLafferty and William M. Foley
United Aircraft Corporation Research Laboratories
Hartford, Connecticut

Work on a vortex-stabilized gaseous nuclear rocket was initiated in 1959 under company sponsorship. Certain phases of this work were supported by Edwards Air Force Base from 1961 through 1963, and continued support of this project has come from the Space Nuclear Propulsion Office since 1963. The Space Nuclear Propulsion Office has also supported the work on the nuclear light bulb which I described yesterday.

Our talk today will be divided into four parts. The first part will deal with a description of the engine concept, and the second will cover a description of our work on radiant heat transfer. The third part will cover the major phase of our work, which is the fluid mechanics aspects of vortex flow, and which is the most crucial problem to be overcome in investigations of a vortex-stabilized gaseous nuclear rocket. Bill Foley will give this third part of our presentation, and Bruce Johnson is here to answer any questions that stump both Bill and me. The fourth part of our presentation will be an attempt to put all of the various technologies together to see what kind of a rocket might be made, what kind of performance it might have, and what conditions we have and have not simulated in our work.

PART I - DESCRIPTION OF ENGINE CONCEPT

The principle of operation of a vortex-stabilized gaseous nuclear rocket can be understood by referring to the first of today's slides, which is UAC Slide 1. The moderator walls form a vortex tube which is symmetrical about the centerline. Hydrogen is injected tangentially near the outer periphery of the tube and spirals radially inward and along the tube until it passes out the annular exhaust shown on one end of the tube. This hydrogen is seeded and heated by thermal radiation from gaseous nuclear fuel which is shown

as an annulus near the centerline of the vortex tube. Our calculations indicate that approximately 1% by weight of seeding material is required in the hydrogen propellant in order to make the propellant sufficiently opaque that the heat transferred to the wall becomes approximately 0.1% of the heat radiated from the nuclear fuel annulus.

The rotational flow within the vortex tube in a full-scale engine will create a centrifugal acceleration of approximately 30,000 g's. This centrifugal acceleration influences three different regions of the vortex tube: the region near the outer wall, the region at the interface between the hydrogen propellant and the nuclear fuel, and the nuclear fuel region itself. In the outer region the centrifugal forces stratify the fluid according to its temperature, causing the cold gases to stay near the wall and the hot gases to stay near the inner edge of the propellant region. This tendency toward stratification also tends to prevent turbulent mixing at the shear interface between the fuel and propellant regions. According to theory, the tendency to overcome unstable Helmholtz waves at this shear interface due to acceleration forces and density gradients is described by the Richardson number. Our theoretical calculations indicate that we should expect laminar flow in this shear region for some conditions as a result of the stabilizing influence of centrifugal force.

In the fuel region, one might normally expect instabilities because the density of the nuclear fuel is obviously greater than the density of the hydrogen propellant at the outside edge of the fuel-containment region. I don't want to get into Bill Foley's presentation too much, but the basic principle is of considerable interest in the radiant heat transfer discussion. In our tests, we cause the simulated nuclear fuel to rotate with less angular momentum than the simulated propellant by injecting the simulated nuclear fuel into the fuel-containment region with little or no angular velocity. The effective density of the fluid is proportional to the product of mass density and centrifugal acceleration. The simulated gaseous nuclear fuel "feels" light because it has low centrifugal acceleration, while the light simulated propellant "feels" heavy because of high tangential velocity and high centrifugal acceleration. Bill Foley will show you movies of heavy gas suspended in a vortex of light gas in Part III of this presentation.

A last point in the description of the engine concept is that vortex flow naturally provides a secondary flow passing down the end walls of the vortex tube. This flow will serve to protect the end walls from axial radiant heat transfer in a full-scale engine. However, it may be necessary to inject additional low-angular-momentum flow in a full-scale engine as shown in UAC Slide 1 in order to provide added protection for the end walls.

PART II - RADIANT HEAT TRANSFER

Our work on radiant heat transfer has included theoretical investigations of the opacity of gases at high temperatures, theoretical calculations of temperature distributions in a gaseous nuclear rocket engine, and experimental investigations to determine the opacity of particle seeds. The theoretical calculations of gas opacity have considered both the opacity of hydrogen and the opacity of nuclear fuel.

Calculation of hydrogen opacity first requires knowledge of hydrogen composition, including the population in all excited states. From calculations of composition we have determined the spectral opacity due to bound-bound transitions, bound-free transitions, and free-free transitions. At low temperatures, the main contributor to opacity over a wide part of the spectrum is the wings of the hydrogen Lyman-alpha line. This result is due to the high pressures of 500 to 1000 atm which we expect to exist within the engine. The high density due to these high pressures spread the Lyman-alpha line over a wide part of the spectrum.

In determining the opacity of gaseous nuclear fuel, we have set up a model fuel atom in which we have assigned ionization potentials and energy levels for excited states. We have calculated the composition of nuclear fuel, including the fraction of the electrons in the different excited states. We have determined the opacity due to bound-bound transitions between different excited states, bound-free transitions from each of these excited states, and free-free transitions. One result of the calculations is that the electron density is sufficiently high to spread out the wings of the lines resulting from bound-bound transitions so that the opacity due to the lines is effectively a continuum. We have used these results both in calculation of spectral radiant heat transfer and of overall radiant heat transfer by techniques which employ opacities averaged over the complete spectrum.

One result of the opacity calculations is that the opacity in the high-temperature region near the center of the vortex tube is extremely high. The average photon mean-free path in this region varies from approximately 10^{-3} cm to 1 cm.

The spectral opacity of hydrogen in the visible portion of the spectrum is negligible at temperatures up to approximately 10,000 R. Therefore, we need some kind of seeding material to make the hydrogen opaque so that it will absorb energy and permit its temperature to be increased to a temperature of approximately 10,000 R. Our calculations indicate that the most desirable seed is composed of a large number of very small particles. These particles must be made of materials which will not combine chemically with

hydrogen, such as tungsten or tantalum. We will discuss measurements we have made of the opacity of particles later in the talk.

Our calculations of temperature distribution in the engine have been made on the basis of a heat balance at each position in the engine. The need for such a heat balance was mentioned in a question raised concerning a preceding paper. In the propellant region, we match the heat deposited by thermal radiation to the heat carried away by convection. In the fuel region, we match the heat carried away by radiation to the heat deposited by the fissioning fuel. This heat deposited by the fissioning fuel is assumed to be proportional to the local density of the fuel.

One result of our calculations is that very high temperatures are encountered near the centerline of the vortex tube due to the high opacity or low photon mean-free-path in the high-temperature region. It is not a matter of creating energy in the center and hoping that this energy will be absorbed before it reaches the wall. Instead, each radial layer within the engine radiates energy to the next layer which absorbs and reradiates the energy to a succeeding layer. This continued absorption and reradiation occurs many times before the energy which is created in the center is transmitted to the propellant region.

The seeding of the hydrogen propellant near the wall does not appear to be the major problem. Our work indicates that 1% by weight of particles will provide an effective absorption coefficient of approximately one reciprocal centimeter. In 10 cm, or approximately 2.5 in., the energy flux may be reduced by a factor of e^{10}. Therefore, it takes very few centimeters of cold seeded hydrogen to substantially reduce the heat transfer to the wall.

Question: What's going down the middle?

Answer: A certain amount of hydrogen will diffuse through the fuel region and come out on the centerline of the vortex tube, although diffusive flow tends to be quite small in an engine of this type. However, in vortex flow there is a substantial amount of secondary flow running down the end walls which has to be pulled out one or both ends of the vortex tube. Our fluid mechanics tests show that the vortex flow in the fuel-containment region is fairly insensitive to whether we take the end-wall boundary layer flow out one or both end walls.

Question: There is a sort of fuelless region in the center?

Answer: There is a fuelless region in the center which you will see in the movies which Bill Foley will show you in a few minutes.

A typical calculated temperature distribution in a full-scale gaseous

nuclear rocket engine is shown in UAC Slide 2. The curve shown on this slide was calculated for a pressure of 1000 atm and a heat flux at the edge of the fuel of one million BTU/sec-ft^2, which is approximately 1000 MW/ft^2. The high temperature near the centerline, approximately 140,000 R, is required by the high opacity of the gases in the fuel-containment region and in the inside edge of the propellant region. The temperature gradient at one point in the propellant region is on the order of a million deg/cm. The reason for this high-temperature gradient is that the hydrogen gas in this region is extremely opaque. The effective radiation thermal conductivity from a Rosseland mean opacity analysis is approximately equal to the ordinary thermal conductivity of copper or aluminum at room temperature, which, with the high heat fluxes in the engine, is practically an insulating value of thermal conductivity. The insulating effect of the low radiation thermal conductivity is the factor which forces the temperature at the centerline to very high values. Once the gases are very hot, they become less opaque for two reasons: the density is decreased, and the spectral heat flux occurs at higher photon energies where the spectral opacity is reduced. In addition, there is the T^3 effect on radiation thermal conductivity. Therefore, once these high temperatures are encountered, the temperature gradients are relatively small.

These high temperatures were very disconcerting when we first obtained results from our temperature distribution calculations, and we checked our calculation techniques very thoroughly. However, the reasoning in which we considered medium-temperature hydrogen as an insulator finally convinced us that such high temperatures were required in a gaseous nuclear rocket engine of this type. For reference, the heat flux at the edge of the fuel region in UAC Slide 2 corresponds to blackbody radiation at a temperature of approximately 40,000 R or 22,000 K.

The temperature distribution can be understood by following a hydrogen fluid element from the outer wall as it is heated by thermal radiation. The hydrogen is injected through the outer wall at a temperature of 4000 to 5000 R after having been used to cool the moderator wall. The temperature rises abruptly to a value of approximately 9000 or 10,000 R as a result of absorption of thermal radiation due to the particles in the hydrogen. As the particles vaporize, the opacity drops and the rate of increase of hydrogen temperature with distance decreases. The resulting plateau is similar to the plateau which Al Kaszak showed you in a preceding paper. At a temperature slightly over 10,000 R, the hydrogen becomes very opaque, and the temperature rises extremely rapidly to a value on the order of 60,000 to 80,000 R. One result of this rapid increase in temperature is that most of the heat which passes across the edge of the fuel region is absorbed in causing the large temperature rise in this region.

Except near the end walls, we assume that the temperature distribution is independent of axial distance. Temperature is assumed to be independent of axial distance because the stratification due to flow rotation will keep layers of the same temperature and the same density at the same radius.

A temperature distribution of the type shown on this slide is calculated by a complicated iterative procedure. In the first iteration, average gas opacities are employed. A diffusion analysis is employed from the centerline of the vortex tube to the radius at which the temperature is on the order of 20,000 R. A transport analysis based on the use of average opacities is used from this temperature to the wall of the vortex tube. We then insert the first calculated temperature distribution in a machine computer program which calculates the spectral heat flux at a number of different wavelengths. This main machine computer program uses the spectral opacity of the gases which are present at each wavelength and at each temperature. It employs a spectral diffusion analysis if the gases are opaque, or a spectral transport analysis if the gases are relatively transparent. This machine program then integrates the total heat flux at each station from the calculated spectral heat flux. By comparing the total heat flux obtained by integrating spectral heat flux and the total heat flux obtained from the analysis using average gas opacities, we calculate a quantity which we call a radiation attenuation parameter which is related to the ratio of true total heat flux to that calculated using average opacities. This radiation attenuation parameter is then used to recalculate a temperature distribution using modified average gas opacities. The temperature distribution shown in UAC Slide 2 was the result of three successive iterations to determine temperature distribution.

The temperature distribution in UAC Slide 2 was calculated on the basis of a radiant heat transfer of 10^6 BTU/sec-ft^2 at the edge of the fuel region, which represents approximately 24 x 10^6 BTU/sec-ft of tube length. The effect of heat transfer rate per foot of tube length on the temperatures at the interface between the fuel and propellant regions and the centerline temperatures are shown in UAC Slide 3. The values from the preceding slide are indicated by the arrow on the abscissa of UAC Slide 3 and correspond to an engine having a thrust-to-weight ratio of 20, a diameter of 10 ft, and operating at a pressure of 1000 atm. It can be seen from this figure that a reduction in heat flux per unit tube length by one order of magnitude causes a reduction in the temperatures in the engine by approximately 30,000 R. It can also be seen that the use of opacities associated with a pressure of 500 atm also causes some reduction in engine temperature.

[redacted]

Let us now consider the opacity of small particles. We express the opacity of small particles in terms of square centimeters per gram. This means that, if a gram of material having fairly large size particles were sprinkled on white paper and a light beam aimed at the particles, the measured area of the particles' shadows in square centimeters would give us this figure of square centimeters per gram. It is obvious that this figure of merit should be as high as possible. The theoretical value of this parameter for graphite particles is approximately 70,000 cm^2/g. The first tests conducted at NASA Lewis with graphite particles suspended in water indicated values of between 6000 and 12,000 cm^2/g, or much less than that indicated by theory. We also conducted tests which indicated low opacities relative to theory. Both we and the personnel at NASA Lewis believe that the reason for low measured opacities is particle agglomeration which causes some of the small particles to hide behind neighboring particles and not provide the theoretical contribution to opacity.

The object of our recent experimental program has been to cause deagglomeration of particles. To do this, we employ the duct arrangement shown in the top of UAC Slide 4. We pass a particle-gas mixture through a series of small holes having diameters of approximately 0.020 in. The resulting particle-gas stream passes through a somewhat larger chamber in which a light attenuation measurement is made. The opacity of the particles is determined from the difference in light transmission with and without the particle-gas stream passing through the light beam.

The extinction parameter of the particles is plotted as a function of pressure upstream of the small nozzle in UAC Slide 4. An increase in pressure causes an increase in velocity for pressures below the sonic pressure ratio, and causes an increase in turbulence at all pressure levels. Shown in this slide are data with nitrogen carrier gas and three different nozzle lengths, and for a helium carrier with one nozzle length. It can be seen that the opacity is increased either by an increase in nozzle length or an increase in velocity as produced by the substitution of helium for nitrogen as the carrier gas.

We plan to conduct additional tests at higher pressures and with longer nozzle lengths in an attempt to provide additional increases in particle opacity. It is interesting to note that recent tests at the NASA Lewis Research Center in which some aerodynamic shear was employed have resulted in their obtaining extinction parameters on the order of 22,000 cm^2/g as compared to between 6000 and 12,000 cm^2/g in their original tests.

Question: Are you talking about metallic particles or nonmetallic particles?

[redacted]

Answer: The particles employed in these tests were graphite because they are easy to obtain. However, in a full-scale engine, graphite would react with hydrogen. Therefore, in a full-scale engine we would have to employ particles made of tungsten or some other high-temperature material.

Question: I had in mind that the opacity would depend on the electrical conductivity of the particles. It makes a difference whether you use a metallic or nonmetallic particle?

Answer: Yes. We are now in the process of calculating theoretical opacities for a number of different particle materials using the Mie theory of scattering. We also plan to conduct tests using different kinds of particles. I believe Bob Ragsdale and Chester Lanzo from NASA Lewis have conducted tests with tungsten particles which gave results which were not too much different from the results for graphite particles.

Question: How big is this small particle?

Answer: We hope to employ particles having radii on the order of 0.10 micron. The nominal size of particles as purchased from a manufacturer is on the order of 80 Å. However, if these particles are observed in an electron microscope, the particle agglomerates are often substantially greater than a micron in diameter. We hope to reduce the average size of particle agglomerates to approximately 0.10 micron.

Question: Don't they vaporize as soon as they get into the hot gas?

Answer: The particles will vaporize when they get to their boiling point which is on the order of 8000 to 10,000 R. Below that temperature, the particles will exist as a liquid, in which stage they should also provide substantial opacity.

Question: Is the molecular conduction of heat due to free electrons a significant effect?

Answer: No. A calculation indicated that molecular thermal conductivity was several orders of magnitude less than radiation thermal conductivity.

Question: I don't understand what you mean by a dashed line indicating theory.

Answer: The dashed line in UAC Slide 4 indicates the results of calculations made using the Mie theory for particles having a diameter of 1000 Å. The experiments were made for a particle-gas stream which contained agglomerates of many different sizes.

Question: What about hydrogen pumping problems?

[redacted]

Answer: The turbopump is a major mechanical problem.

Question: What pressure did you have?

Answer: For 1000 atm pressure in the cavity, the pressure at the pump exit is on the order of 1300 atm.

PART III - FLUID MECHANICS

Our fluid mechanics work involves only low-temperature fluids and is designed to demonstrate satisfactory heavy-gas containment at the density ratios that would be present in a full-scale gaseous core nuclear rocket. As an introduction, I want to present a short description of our test equipment and our test techniques. After that I will discuss the flow patterns which we observe in vortex chambers, before showing some iodine containment movies and telling you about the present test program which we have underway. Some of the work that I will discuss, such as the description of flow patterns, is going to be "old hat" to some of you since it is based on results obtained a couple of years ago. However, because of the relatively diverse backgrounds of this group, I thought that presentation of these other results would pave the way for discussions of what we are doing in our present test program.

The geometry of the vortex tubes which we use in the laboratory is like the geometry of the vortex chambers for the rockets described by George McLafferty. As shown in UAC Slide 5, two different configurations are used; one we call the basic vortex tube and the other the axial-flow vortex tube. In the basic configuration, a large mass flow is injected through a single slot that extends the full length of the peripheral wall of the vortex tube; most of this flow swirls around and is removed after one revolution through a bypass screen. The remainder of the fluid spirals inward and is removed through thru-flow ports located at the center of each end wall. We use this arrangement because it allows independent adjustment of the tangential Reynolds number and the radial Reynolds number of the flow. When we want to test something that more closely simulates the geometry of a full-scale rocket, we go to the axial-flow configuration; the flow is injected in the same way as for the basic configuration, but none of the flow is removed through the bypass screen. Instead, all of the flow which would otherwise be bypass flow is withdrawn axially through an annular exhaust port in one end wall. Note that r_1 in UAC Slide 5 is the outer radius of the vortex tube. This is the dimension which is used in the nondimensionalization of our test data. The vortex tube length is six times this radius.

[redacted]

The iodine injection duct, shown in UAC Slide 5, illustrates one location which has been employed for iodine injection. With this configuration, iodine is injected radially through a single duct in the peripheral wall and falls radially inward and is trapped in an annulus near the center of the vortex. We have also run tests in which iodine and other heavy gases have been introduced in a number of other ways, such as through various stations in the end walls and through a porous tube that runs the full length of the vortex tube along the centerline.

Question: Is that slot extending over the full length of the vortex tube?

Answer: Yes, it runs the full length. It is a continuous, uninterrupted slot. The same thing is true with the bypass screen. It is a screened area that runs the full length of the tube and is used to remove flow after one revolution. This skims off the peripheral wall boundary layer.

Our tests fall into two categories. One category is the type of test where we are simply trying to learn what flow pattern one obtains in vortex tubes like these if fluid is injected and removed in the described manner. Now, as you might suspect, this will not necessarily produce the characteristics that are desired insofar as heavy-gas containment is concerned. Consequently, we have also conducted tests which fall into a second category where we attempt to modify the vortex so that it has the desired characteristics. This is accomplished by a variety of techniques, such as varying the effective skin friction of the end walls and introducing secondary jets through the end walls. Many of our tests have been run using water as the working fluid because the time scale in which the various phenomena occur is much longer with water than it is with gases. Also, flow visualization is much simpler with water than with a gas. Of course, when it comes to containment, we have to work with gases.

As those of you who have worked with rotating flows know, any probe which is introduced into the flow produces a disturbance which creates a convective cell. Therefore, except in the end-wall boundary layers, we have not used the usual probe techniques that are common in hydrodynamics. Instead, we have had to resort to the use of neutrally buoyant particles and dye as tracer materials. UAC Slide 6 is a photograph of some of these neutrally buoyant particles in rotating flow. They are illuminated with a chopped light beam so that they appear as a series of dashes on a time exposure. By counting the number of dashes and measuring the radius of the particle orbit, the circumferential velocity can be determined. From the pitch of the helices and the circumferential velocity, the axial velocity can also be determined. We have used this technique to map the flow fields within vortex tubes for quite a number of flow conditions. Of course, many

of the particle traces cannot be used for evaluating the local velocity since they noticeably change radius during one revolution. We use only particles which move in a constant-radius orbit.

Dye trace techniques, which are illustrated in UAC Slide 7, have also been very helpful in determining the flow field characteristics. This is a photograph of dye which has been injected into the basic vortex tube through both end walls. The dye near the right end wall was introduced considerably before the dye near the left end wall. As you can see, the dye is distributed in sort of funnel-shape patterns. Note that the boundaries of the dye front near the right end wall and the small front near the center of the vortex tube are very well defined and are laminar in appearance. The dye near the left end wall, which has been introduced much more recently, is at a larger radius and is in the process of moving radially inward to take on a pattern like the right pattern. The left pattern is much more diffuse because it is near the outer radius of the vortex tube where the turbulence level is high. We would envision containing the heavy nuclear fuel (in a full-scale rocket) in the central region of the vortex where the well defined, laminar dye patterns form. Similar results to those obtained with dye in a water vortex have also been obtained by introducing smoke into air vortexes. Also, on a few occasions, we have even gone so far as to introduce helium-filled soap bubbles into an air vortex to obtain results similar to those shown for plastic particles in a water vortex. This is a very cumbersome technique, however, and has not been used to any extent.

The data from the particle- and dye-trace techniques can be used to map the flow field, as shown in UAC Slide 8. The lines in this slide are not actually streamlines; they are the cross sections of stream sheets. However, for convenience I will refer to them as streamlines. If a substantial fraction of the injected flow is removed through the ports at the center of each end wall (i.e., as thru-flow) a streamline pattern like that shown in the upper sketch is obtained. Note that although the thru-flow is ejected along the entire length of the vortex tube, a major portion of it runs over to the end walls, enters the end-wall boundary layers, and is carried radially inward along the end wall and out through the thru-flow ports in the end walls. Only the flow introduced at the very center of the vortex tube actually passes all the way to the center through the main vortex flow. This characteristic of most of the flow entering the end-wall boundary layers is typical of vortex tubes over a wide range of operating conditions. If the circumferential velocity at the outer radius of the vortex is held constant and the thru-flow is reduced to a small value, a streamline pattern like that shown in the lower portion of UAC Slide 8 is obtained. In this case, all of the radial flow will enter the end-wall boundary layer at some point. Near

the center of the vortex tube some of the flow leaves the boundary layers and flows radially outward setting up the convective cell.

Question: You have high ratios of tangential to radial Reynolds numbers?

Answer: Yes, the tangential Reynolds number is about 1000 times the radial Reynolds number, based on the velocities at the periphery of the vortex tube, for the lower sketch in UAC Slide 8. The local radial Reynolds number in the central region of the vortex goes to zero at one radius and then becomes negative within part of the vortex.

The reason for the convective cell is very simple. The flow that is adjacent to the end walls is slowed down by the end-wall shear. The flow in the central region of the vortex has a substantial radial pressure gradient which balances the centrifugal force acting on the fluid elements. Since the boundary layer is thin, the same radial pressure gradient exists there as in the central vortex; and the slow moving boundary layer flow is accelerated radially inward. Once all of the radial flow has entered the end-wall boundary layer at some radius, shear also becomes very important in the central vortex. As a result, the radial pressure gradient changes so that at an inner radius there is no longer sufficient pressure gradient to continue accelerating the boundary layer flow. Boundary layer outflow then occurs, and a convective cell is established. The next two slides help to illustrate this process in greater detail.

UAC Slide 9 illustrates typical boundary layer profiles obtained by pitot probe techniques. On the left is a sketch of the circumferential component of velocity plotted against distance from the end wall, and on the right is a graph of the radial velocity plotted against distance from the end wall. The circumferential velocity has a boundary layer profile very much like that which is obtained for a flat plate. However, the distribution of the radial component of velocity is quite different. Near the wall the velocity rapidly increases from zero to a very high velocity. At greater distances from the wall, it slowly decreases to the free-stream radial velocity at the outer edge of the boundary layer, which is usually very small. Note in particular that the maximum radial velocity is of the order of the tangential velocity, which explains why so much mass flow is carried inward through the end-wall boundary layers.

If one calculates what the boundary layer, or secondary, mass flow distribution will be for a low radial Reynolds number, you obtain a result like that in the upper curve shown in UAC Slide 10. The mass flow increases with decreasing radius until a maximum is reached and then decreases again near the center of the vortex tube. One of the big surprises

to us when we calculated the mass flow distribution was that our calculations kept indicating that for some cases there was more flow in the boundary layer than the total flow injected at the periphery of the vortex tube. This did not seem plausible until we constructed streamline patterns like that shown in the lower half of UAC Slide 10. Then the reason for the large mass flow at intermediate radii became obvious. A cell forms which contains a substantial amount of trapped fluid that continuously recirculates. Recirculation cells of this type occur in vortex chambers for a wide range of operating conditions. These recirculation cells are undesirable since they convect fluid axially from the central region of the vortex tube to the boundary layers. If an attempt is made to contain a heavy gas within the cell, sufficient mixing occurs in the end-wall boundary layers to lose a substantial amount of the heavy gas. Consequently, we would like to eliminate or at least control the axial convection so that it does not cause a high fuel-flow rate. As a result, we have devoted considerable effort to the control of end-wall boundary layers in an effort to achieve more desirable vortex flow patterns.

The upper sketch in UAC Slide 11 illustrates one such desirable flow pattern. First, since an end-wall boundary layer always forms, most of the radial flow would be allowed to enter the end-wall boundary layer at a large radius. The problem is then to keep this flow in the boundary layers so that a convective cell does not form. If one adds sufficient friction in the proper distribution to the end wall, this result can be achieved. Then, only the flow injected near the axial midpoint of the tube would flow through the fuel-containment region and at a very slow inward velocity. The axial velocities in the fuel containment region would be zero. In fact, it may even be desirable to reverse the direction of flow in the central region of the vortex by putting the fuel in along the centerline and letting it move radially outward. I would like to return and discuss the lower sketch in UAC Slide 11 later.

We have devoted a considerable amount of effort, both theoretical and experimental, to the control of end-wall boundary layers. In the tests that we ran initially, we introduced the additional skin-friction by installing protruding rods on the end wall. More recently, we have used distributed suction on the end walls. Neither of these techniques are proposed as suitable means for controlling the end-wall boundary layers in a full-scale rocket. Because of the problem of cooling the end walls on a rocket, injection boundary layer control will be required. However, the distributed friction and suction techniques are simpler to employ. Since we wanted only to demonstrate that the desired flow characteristics can be achieved, the simplest control techniques have been employed.

[redacted]

UAC Slide 12 is a photograph of a dye pattern in the basic vortex tube with distributed-friction flow control. Just seconds before the photograph was taken, dye pulses were injected from both end walls. They are visible as diffuse dye clouds near both end walls. UAC Slide 13 is a photograph of the vortex tube nearly an hour later. Clear water has been injected continuously at the outer periphery during the entire period and withdrawn from the ports in either end wall. No more dye has been added. The dye has very slowly been diffused or convected toward the center of the vortex tube so that the entire central region now contains some of the dye. This central region of the tube obviously has at most a very slow convective velocity or this dye would not have been trapped there for an hour in such a large annular region. Actually, we have waited for an afternoon and still had a large cylindrical dye region within the vortex tube at the usual operating condition of a tangential Reynolds number of 70,000. It is particularly interesting to note that even near the end walls the dye has not been convected from the vortex.

Question: This is all the same density, is it not?

Answer: Yes, this is a constant-density flow. The water vortex tests are only to determine streamline patterns and to determine what can be done to alter these patterns.

May I return again to UAC Slide 11. The lower sketch illustrates a typical streamline pattern in the axial-flow vortex tube determined by particle-trace techniques. Most of the injected flow is removed through the annular exhaust port in the right end wall, and only a small amount is withdrawn through the ports at the center of each end wall. The flow introduced near the left end wall runs into the left end-wall boundary layer. However, over most of the length of the vortex tube, the flow turns toward the right end wall and is carried out through the annular exhaust port. A small amount of flow at the right end wall enters the end-wall boundary layer just inside the radius of the exhaust port and then comes back out of the boundary layer and forms a counterflow region. Some of this counterflow actually travels the length of the vortex tube and enters the end-wall boundary layer on the left end wall. Just as in the basic vortex tube, the flow pattern in the central region of this vortex tube is quite complicated, but it is important to note in particular that the region of high-axial-velocity flow toward the axial-flow end wall is confined to the outer portion of the vortex tube. The central region of the vortex again contains low axial velocities, although they are somewhat higher than in the basic vortex tube at equal tangential and radial Reynolds numbers.

UAC Slide 14 is a photograph taken of the axial-flow vortex tube

[redacted]

immediately after dye has been introduced through the peripheral wall at the axial midplane. The annular exhaust port is on the right. Most of the dye is very rapidly convected to the right end wall by the flow that leaves the tube through the annular exhaust port. A minute later, as shown in UAC Slide 15, much of the dye that was in the region of high axial velocity has been carried out of the vortex tube. However, a well-defined inner dye annulus can be observed which is moving from right to left. This inner dye cell is formed by the counterflow that I mentioned previously. Note that the leading and inner edges of the dye cloud are well defined and have the laminar appearances of the dye patterns that were observed in the basic vortex tube. The outer edge of the dye cloud near the axial midplane is diffuse in appearance, and many small filaments can be observed. These filaments result from the radial movement of some of the counterflow into the turbulent outer region of flow moving toward the axial-flow end wall. We have not as yet attempted to control the end-wall boundary layers in the axial-flow vortex tube. It is expected that in the near future an attempt will be made to control the boundary layer flow in this tube and thus reduce the velocities in the counterflow region.

This concludes my brief review of typical results we have observed in water vortex flows. Now I would like to go on and describe some of the gas vortex tests. In these tests, iodine and mixtures of iodine and freon are introduced into the vortex flow to determine how much heavy gas can be contained within a light-gas vortex.

The next slide, UAC Slide 16, is an end view of an air vortex into which iodine has been injected. A well-defined iodine annulus can be observed near the center of the picture; and outside of this annulus, the peripheral wall of the vortex tube can be seen. The iodine which is contained within the vortex has been injected through a single injection duct located in the periphery of the vortex tube. The annular iodine distribution is typical of the patterns usually observed, and the density is often quite uniform over the full length of the vortex. The annulus results from iodine becoming trapped in one of the recirculation cells which were observed in the water vortex tests. Since the velocities are very low within the cell, the iodine remains for a considerable period of time.

Now I would like to show a movie which shows more clearly the typical behavior of a light-gas vortex when a heavy gas is injected into it. These photographs show how an annular distribution of heavy gas occurs once the heavy-gas injection has commenced and how the heavy gas is visible for nearly a minute once the injection has ceased. Injection of the heavy gas with either too little or too much radial momentum results in excessive loss rates.

In our gas-vortex test results, a heavy-gas time constant is defined. It is the number of pounds of heavy gas stored within the vortex, divided by the steady-state feed rate in pounds per second which was used to achieve this heavy-gas storage within the vortex. Thus, the time constant is a measure of the frequency with which the stored heavy gas is replaced by the injected flow. With our iodine-helium tests, the time constant is on the order of 1/2 to 1-1/2 sec, and with an air vortex it is on the order of 4 to 12 sec. These facts are illustrated in UAC Slide 17. (The row labeled "dye, H_2O" should be neglected for the present.) If one calculates either the time constant for the iodine if it is convected or if it is diffused radially out of the vortex, you find that both are proportional to the density of the fluid in the vortex, ρ_1; the square of the radius of the vortex tube, r_1; and the reciprocal of the viscosity. This fortunate result is true only because the viscosity and diffusivity differ only by a constant. For iodine-helium tests, the value of this grouping of terms--shown in column 3 of UAC Slide 17--tends to be on the order of 60; it is on the order of 500 for the air-iodine tests. If the time constant is really proportional to $\rho_1 r_1^2/\mu$, then the ratio of the measured time constants to the value of this parameter should yield the same nondimensional time constant, τ, regardless of the gases employed. The data shown in the fourth column indicate that indeed both helium and air tests lead to the same nondimensional time constants even though the dimensional times differ by almost an order of magnitude. The visually observed residence time of dye in the water vortex tube is of the order of 1000 to 4000 sec or longer. This is illustrated in the third row of data presented in UAC Slide 17. The value of the $\rho_1 r_1^2/\mu$ parameter for water is 16,000--30 to 300 times the value for air and helium. When the dye residence times are nondimensionalized by dividing by $\rho_1 r_1^2/\mu$, the resulting nondimensional time constants are three to ten times longer than those for the gas vortex tests. As illustrated during the movie, the observed iodine residence times are three or more times longer than the measured time constants. Thus, the values of the nondimensional time constants for water, air, and helium are comparable. This, we feel, lends some credence to the use of the $\rho_1 r_1^2/\mu$ parameter to nondimensionalize the time constant data.

The next slide, UAC Slide 18, shows a typical plot of iodine weight flow against time in an air vortex. The weight flow rates are determined by passing light beams through the ducts which carry flow from the vortex tube and measuring the light absorption which occurs due to the presence of the iodine in the gas streams. In taking such data, we first set up the vortex flow without iodine injection. Then the iodine is turned on at the time marked zero. One has to be careful because the very fact that there is injection of iodine changes the characteristics of the vortex. Consequently, injection is continued until the outflow of iodine from the vortex is equal to the inflow and the

amount of gas being lost through the bypass and the thru-flow ports is constant in time. The injection is then turned off, as noted on the slide. We do not care what transient flow condition the vortex goes through after the iodine injection is turned off since the data obtained after shut-off are used only to determine the gross amount of stored iodine within the vortex. The total amount of stored iodine is determined by integration from the weight flow-time trace after iodine shut-off. The time constant is then evaluated by dividing the amount of iodine stored within the vortex by the feed rate required to store that much iodine within the flow. UAC Slide 19 contains some typical nondimensional time constants obtained in this manner for an air vortex.

This slide contains time constant data obtained for a wide range of test conditions in the basic vortex tube. The density ratio, which is plotted on the horizontal scale, is the average density of the iodine within the entire annular region of the vortex in which we observe the iodine to be contained divided by the density of the light gas just outside this annular region. For tests with an air vortex, plain end walls, and iodine or a mixture of iodine and freon as the heavy gas, the dimensionless time constants were on the order 0.02 to 0.03 at the density ratios we were able to achieve (i.e., less than one). It should be pointed out that in tests with iodine and freon, the iodine was used only as a tracer to permit detection of the heavy gas by optical techniques. Because of the short residence time of this gas mixture and the small pressure gradient within the vortex, the iodine and freon were assumed not to separate. Both gases were included in evaluating the density ratios. When the light gas was changed from air to helium, the time constant decreased. However, we did not run many tests with helium and plain end walls because at that time we were concerned more with controlling the flow by use of the distributed friction technique, which has already been discussed. This technique appeared to offer a great deal of promise for improving the density ratio. As may be seen from UAC Slide 19, it was possible to increase the density ratio by use of the distributed-friction end walls to about two and a half in a helium vortex without any decrease in the time constants from those values achieved with air.

Question: Could you reiterate what that density ratio is--because it is important that they understand it?

Answer: Yes, the heavy-gas density, $\bar{\rho}_{F_6}$, is the average density of the heavy gas within the entire annular region in which the heavy gas is observed. We divide the total mass of heavy gas stored within the vortex tube by the volume of the observed annular region to get this average density. The average heavy-gas density is then divided by the density of the light gas, ρ_6, which

[redacted]

was injected into the vortex tube to obtain the density ratio plotted in UAC Slide 19. The peak density ratio at some radius is probably much greater than the value of the average density ratio for each of these cases.

Question: What is the density ratio of the iodine to helium? Is that really a large amount?

Answer: If you are asking for the density ratio of pure iodine to pure helium this ratio would be about 63.5.

UAC Slide 20 illustrates the effect of a superimposed outer region of high-velocity axial flow on the time constant. All of the data have been obtained in an air vortex. In this slide, the velocity, V_z, is the average axial velocity of the flow in the annular exhaust slot; and V_ϕ is the tangential velocity at a radius equal to eight-tenths of the vortex tube radius. The data for $V_z/V_\phi = 0$ were actually obtained in the basic vortex tube and are shown for comparison. When flow is withdrawn through the annular exhaust slot there is a decrease in the time constant by about a factor of two. However, it should be noted that a considerable amount of time has been devoted to obtaining large time constants in the basic vortex tube while very little time has been devoted to optimizing the test conditions in the axial-flow vortex tube. For example, we have done nothing to control the end-wall boundary layers in axial-flow vortex tubes. It is important to notice that data have been obtained at two tangential Reynolds numbers, 40,000 and 70,000. Within the scatter of the data there is no difference in time constant for these two Reynolds numbers. However, a vortex-stabilized gaseous core nuclear rocket may require tangential Reynolds numbers up to a million. It remains to be seen what happens when we operate at these high Reynolds numbers.

An axial-flow Reynolds number, Re_z, which is related to the tangential Reynolds number, will be used subsequently. It is the tangential Reynolds number, Re_t, multiplied by V_z/V_ϕ (i.e., $Re_z = Re_t \times V_z/V_\phi$).

This summarizes the main results that I want to present today. No high-temperature vortex test data have been presented. Such data have been omitted for two reasons. First, the tests that we have run with a superimposed radial temperature gradient did not give us the temperature distribution that we desired. Second, temperatures that we have been able to achieve are too low to establish the conditions in which radiation is the dominant mode for heat transfer. As George McLafferty has pointed out, the predominant heat transfer mechanism in a full-scale nuclear rocket is radiation, and some of the stability problems which we would like to study cannot be adequately investigated without simulation of the radiant heat transfer. We feel that the radial temperature gradient will have an important influence on the fluid dynamics of a full-scale rocket, but this means very,

[redacted]

very high temperatures if we wish to investigate such effects. As yet we have not seen fit to complicate our problem to this degree when there are so many other questions which require answers.

Before turning the meeting back to George McLafferty, I would like to summarize briefly our present test program. Both water and gas vortex tests are being continued. The tangential Reynolds numbers will be increased to more than 250,000 during some tests. Also, the V_z/V_ϕ ratio will be increased to a value near one for some tests. Tests using suction boundary layer control on the end walls of the basic vortex tube have been in progress for some time, and in the near future we intend to apply suction to the end walls of the axial-flow vortex tube. That summarizes our present test program. Are there any questions regarding the fluid mechanics?

Question: Doesn't Langmuir show that heavier material has to go to the center of the vortex?

Answer: This can happen, but it is not generally true. If the heavy-gas distribution is determined by convection, then it is possible for the secondary flow to convect the heavy gas to the center. If the flow of the heavy gas is determined by diffusion, then the heavy gases tend to move radially outward. In a two-dimensional, pure vortex--where the velocity varies as 1/r--it turns out that no heavy gas can be contained because the flow is unstable.

Question: Would you obtain longer residence times of the heavy gas if it had a lighter molecular weight?

Answer: Not necessarily. For most operating conditions the heavy-gas loss rate is determined by convection, not diffusion. Consequently, the loss rate may be independent of the density of the heavy gas.

Question: What would happen if you put a light molecular weight gas into the center of your vortex? Would it reside there longer than a heavy molecular weight gas? What is your prediction?

Answer: The central region of the vortex tends to have very high convection velocities which feed the thru-flow ports. The molecular weight of the gases in this region probably would have very little influence on their residence times.

Question: Do you have any experiments in which you inject air through the longitudinal slot at the periphery and inject helium at the center?

Answer: No, we do not have tests of this type.

Question: You haven't tied down the degree of turbulence which you have in your experiment. It is hard to tell from the pictures whether it is laminar or turbulent.

[redacted]

Answer: We have no direct measurements, but we have tried to infer from the dye diffusion photographs what the turbulence level is. If you calculate from the rate of spreading of dye filaments what the viscosity is, it turns out that, for some cases, the eddy viscosity is of the order of 1% of the laminar viscosity. These low values occur for a very weak vortex. The turbulence level varies with the vortex strength and is much higher for a strong vortex.

Question: In a sense, can you say that Taylor instability is negligible in your system?

Answer: No, Taylor instabilities are what make the outside of the vortex very turbulent, but Taylor stability is what makes the inside very laminar. This is because the velocity distribution in the boundary layer adjacent to the peripheral wall is very unstable, whereas the velocity distribution in the central region of the vortex is stabilizing.

Question: When the time constant is defined on the basis of the parameter $\rho_1 r_1^2/\mu$, does this assume a constant Reynolds number?

Answer: Yes, the results should be compared at equal tangential and radial Reynolds numbers.

Question: Yes, but you are interested in going to higher Reynolds numbers so the time constant should change.

Answer: We can't infer anything about the dependence of time constant on Reynolds number from the $\rho_1 r_1^2/\mu$ parameter. However, the tangential Reynolds numbers have been varied from 40,000 to 70,000 without any observed change in the time constant.

Question: What r^2 correlation do you have for your time constant data?

Answer: We have essentially no correlation for air tests. However, for dye residence tests we have compared the results from a 4-in. vortex tube and a 10-in.-diameter vortex tube with good correlation.

Question: Is it true that when you inject dye at the center your time constant is much shorter?

Answer: Not necessarily. It depends on both the flow condition and the method of injection. For instance, in some tests with the suction end walls, flow was injected at the centerline of the vortex through a porous tube, and this has led to some of the best time constant data obtained to date.

Question: You did have a movie with central injection, didn't you?

Answer: No, in this case the flow was injected through a single duct at the axial mid-plane of the vortex, not at the rotational centerline. The resulting

[redacted]

time constants with this injection configuration were very sensitive to the momentum of the injected flow. If the flow was injected with too little momentum, it was immediately swept out through the bypass. If it was injected with too much momentum, it penetrated through the central cell region and into the very center of the vortex where the high convective velocities swept it out of the vortex tube very rapidly. A similar thing happens when one injects through the end walls. With too little momentum the flow is immediately swept into the end-wall boundary layer and out. With too much momentum it creates excessive turbulence and is lost. Considerable optimization is required in finding a suitable injection configuration and condition. We have been able to inject at several points and get similar time-constant results after going through a rather time-consuming optimization process.

PART IV - ENGINE PERFORMANCE

We have now discussed the radiant heat transfer and fluid mechanics phenomena which influence the performance of a vortex-stabilized gaseous nuclear rocket engine. In the following discussion we will attempt to integrate the results of these studies to determine the characteristics of a full-scale engine and to determine what quantities we have and have not simulated in our tests. It will be assumed in most of the discussions that the following are desirable performance goals for a gaseous nuclear rocket engine: a specific impulse of 2500 sec, an engine thrust-to-weight ratio of 20, and a ratio of propellant flow to fuel flow of 1000. We will now discuss the characteristic which we must simulate in order to provide this performance.

We show in UAC Slide 21 a typical gaseous nuclear rocket engine configuration. The length of the engine cavity is approximately 10 ft, and the diameter of the engine cavity is approximately 7.5 ft. The nominal external diameter of the engine is 10 ft, although we now believe that the external diameter should be somewhat larger than this value to permit use of a moderator having layers of different moderator materials. The assumed pressure within the engine is 1000 atm.

The weight of the engine configuration shown in UAC Slide 21 would be approximately 170,000 lb. For our assumed thrust-to-weight ratio of 20, the resulting thrust, F, would be 3.4×10^6 lb. If our assumed specific impulse of 2500 sec is divided into this thrust, the resultant required hydrogen flow, W_H, is 1350 lb/sec.

The total amount of power required to raise 1350 lb/sec of hydrogen to a temperature where it will produce a specific impulse of 2500 sec is approximately 285,000 MW. Approximately 90% of this energy is deposited

[redacted]

in the fuel region by fission fragments and is radiated out by thermal radiation to the propellant. The other 10% of the energy created is deposited in the walls by neutrons and gamma rays. The heat deposition rate per unit volume in the moderator-reflector near the inside surface of the cavity is much greater than that near the outer portion of the moderator.

Question: What basis did you have for selecting thrust-to-weight ratio?

Answer: Our economic studies indicate that such a thrust-to-weight ratio would be very acceptable. We could also probably accept ten-to-one thrust-to-weight ratio or even five-to-one thrust-to-weight ratio, but there would be some loss in the economics of space flight due to such reduced thrust-to-weight ratios.

We have conducted analyses to determine any limitations on engine performance resulting from the necessity of removing the heat deposited within the moderator wall. These calculations indicate that the coolant passages should have diameters on the order of 0.020 in. and that their volume should be on the order of 5 to 10% of the moderator volume. The resulting pressure drop in the moderator is on the order of 10 atm, which seems reasonable.

Our present calculations indicate that the most desirable fuel for use in an engine of this type is plutonium. Our calculations also indicate that the critical mass within this cavity should be approximately 7.5 kg or approximately 16.5 lb. We believe that the fuel region is a larger fraction of the cavity region than is assumed in studies at NASA Lewis. Therefore, there is less fuel compression effect on criticality than in some of the results of the NASA Lewis studies.

If the critical mass of 16.5 lb is distributed uniformly throughout the cavity, the resulting average fuel density, $\bar{\rho}_{F_1}$, is 0.035 lb/ft^3, which is about half of the density of the air in this room. We have assumed in our calculations that the radius of the fuel-containment region is three-quarters of the tube radius, or the volume of the fuel-containment region is approximately 56% of the inside volume of the vortex tube. Therefore, the density based on this fuel volume, $\bar{\rho}_{F_6}$, is 0.062 lb/ft^3.

As I mentioned before, our goal for fuel containment is to have a fuel flow equal to or less than 0.1% of the hydrogen flow. Max Hunter would like this figure to be 0.01%, but let's be conservative for now and aim at a ratio of hydrogen flow to fuel flow of 1000. For this ratio, the fuel flow would be 0.1% of the hydrogen flow of 1350 lb/sec, or 1.35 lb/sec. The corresponding fuel time constant, which is the number of pounds stored divided by the fuel flow rate, is 12 sec, which is almost identical to the time constant that was in the movie which Bill Foley showed you a few minutes ago. Therefore,

[redacted]

we would have to supply fuel at a rate which would replace the critical mass roughly every 12 sec. This would appear to be acceptable on the basis of our economic studies. It is not as good as Max Hunter's "transportation" figures, but it is a long way from his "ammunition" figures.

Although most people consider that hydrogen is the only possible propellant for gaseous nuclear rockets, we are going to consider a number of different possible propellants in the following discussion. We will also assume that any of these propellants can be used to provide a specific impulse of 2500 sec. Let's omit for now the discussion of just how this would be obtained and concentrate our attention on other characteristics of the engine.

Consider the density ratio requirements of a gaseous nuclear rocket engine, that is, the ratio of the average fuel density for criticality to the density of the propellant at the outside edge of the fuel-containment region. Such density ratios are shown in UAC Slide 22. Shown on this figure are values of the density of various propellants at a pressure of 1000 atm and a temperature of approximately 100,000 R, which is the temperature expected to exist at the outside edge of the fuel-containment region according to our studies. If the average fuel density of 0.062 lb/ft^3 is divided by the hydrogen density at Station 6, 0.0065 lb/ft^3, the resulting required density ratio is 9.5. Theoretically, we should be able to raise this density ratio considerably higher than 9.5 if we can avoid instabilities in the flow. However, the maximum value we have obtained in our model tests is 2.2. Therefore, the density ratio required for an engine with hydrogen propellant is greater than we have now simulated.

The density ratios required for water and ammonia rockets are approximately equal to those which we have measured in model tests, and we have almost simulated the density ratio required for a rocket with methane propellant.

Question: Will you repeat again what that density ratio is.

Answer: The numerator in the density ratio is the average density of nuclear fuel required in a volume of 56% of the cavity volume in order to make the engine critical. The denominator in this density ratio is the density of the propellant at the temperatures existing at the outside edge of the fuel-containment region. As we mentioned before, we rotate the heavy gas slowly so that it feels light, and the light gas rapidly so that it feels heavy.

Question: How do you control the rate of rotation?

Answer: We inject the light gas at high tangential velocity and the heavy gas at low tangential velocity.

[redacted]

Question: What keeps the angular momentum of the fuel at a low value?

Answer: Since the flow is quite laminar, it takes quite a bit of time for the heavy gas injected at low angular momentum to speed up from the shear of the high-angular-momentum light gas. Therefore, the average angular momentum of the fuel stays low during its dwell time within the vortex.

Question: Wouldn't the density ratio be dependent on the molecular weight ratio to a certain extent?

Answer: Yes, but we do not have answers on that question yet.

Question: What happens if the critical mass is doubled?

Answer: The required density ratio is doubled.

The effect of engine diameter and pressure level on the required fuel density ratio is shown in UAC Slide 23. It can be seen that an increase in diameter from 10 to 15 ft will result in a reduction in the required density ratio by a factor of approximately two.

Let us now look at time constant requirements. As noted in UAC Slide 21, a time constant of 12 sec would provide a ratio of propellant flow to fuel flow of 1000:1 for the engine shown on that slide. To find the nondimensional time constant, we divide the actual time constant by the parameter $\rho r_1^2/\mu$, which has the units of seconds. The resulting required dimensionless time constants are shown on UAC Slide 24 and vary from 0.056 for hydrogen propellant to 0.010 for water propellant. As noted in Bill Foley's presentation, the time constant measured in the model tests varied from 0.005 to 0.030. Thus, the dimensionless time constants measured in our tests are sufficient to provide a ratio of propellant flow to fuel flow of approximately 1000:1 in rockets with water, ammonia, or methane propellant. However, the highest time constants measured in the tests are only half of those required for a hydrogen rocket having a nominal engine diameter of 10 ft.

The effect of nominal engine diameter on the dimensionless time constant required to obtain a ratio of propellant flow to fuel flow of 1000:1 is shown in UAC Slide 25. It can be seen that an increase in size results in a considerable decrease in the required dimensionless time constants.

The effect of engine diameter on the axial-flow Reynolds numbers in a vortex tube is shown in UAC Slide 26. This axial-flow Reynolds number is defined as the product of the density of the light gas at the edge of the fuel-containment region, the average axial velocity in the propellant region, the ratios of the vortex tube, and the reciprocal of the viscosity of the light gas

[redacted]

at the edge of the propellant region. It can be seen from this slide that a nominal engine diameter of 10 ft is associated with an axial-flow Reynolds number of approximately 10^5 for hydrogen propellant, and approximately 4×10^5 for water propellant. These Reynolds numbers are considerably higher than the axial-flow Reynolds numbers of approximately 15,000 which we have employed in our model tests. So, as Bill Foley said, one of our primary objects is to obtain the test data at higher Reynolds numbers. Such tests will probably require considerable work on vortex flow control methods in order to maintain the same time constants and density ratios at high Reynolds numbers that we have measured at low Reynolds numbers.

Let us now discuss the possible values of specific impulse which can be obtained by the use of different propellants. Up to now we have assumed that 2500 sec is obtainable with any of the propellants listed in our table. This assumption requires some discussion. In UAC Slide 27 we have repeated much of the engine outline which was given in UAC Slide 21. Let us fix the maximum propellant injection temperature at 5300 R, which fixes the propellant injection enthalpy at the values shown in the second column of UAC Slide 27. Since approximately 10% of the energy release is deposited in the wall and 90% is deposited within the cavity, the exit enthalpy is approximately ten times the enthalpy of the propellant injected into the vortex tube. The specific impulse shown in the last column in UAC Slide 27 was obtained from the exit enthalpy using an ideal nozzle coefficient of 0.8. The resulting values of specific impulse vary from 2500 sec for hydrogen to 1200 sec for water.

The specific impulse of 1200 sec shown for a water rocket is only marginally better than that obtainable from a solid-core nuclear rocket. The question now to be answered is how to raise the specific impulse. One method of raising the specific impulse was mentioned in Max Hunter's talk of yesterday in which space radiators are employed to reject part or all of the energy deposited in the wall. In UAC Slide 28, we show the effect of the addition of a space radiator to the specific impulse and thrust-to-weight characteristics of a gaseous nuclear rocket engine. The thrust-to-weight is computed on the basis of the sum of the weight of the engine and radiator. It was assumed in constructing this figure that all engines produce the same total power, so that the thrust-to-weight ratio of the water propellant engine is slightly more than twice as great as the thrust-to-weight ratio of the hydrogen propellant engine. If we had an infinite radiator temperature, we'd have the result indicated by the dotted line on UAC Slide 28. Curves are also shown for assumed radiator temperatures of 2000, 4000, and 6000 R with an assumed radiator specified weight of 1 lb/ft^2.

[redacted]

The requirement for the use of space radiators is normally considered as one of the reasons why low thrust-to-weight ratios are obtained from electrical propulsion engines. However, several points should be made in this regard. First, the energy which must be removed from the space radiator in an electrical propulsion engine is approximately ten times the energy in the exhaust beam. However, in a gaseous nuclear rocket engine, the energy is approximately one-tenth of the energy in the exhaust flow. Therefore, the amount of energy which must be rejected in a gaseous nuclear rocket engine for the same engine thrust and specific impulse is approximately 1% of that for an electrical propulsion engine.

The second point to be considered is that electrical propulsion engines must operate for periods of years, while a gaseous nuclear rocket engine on a round-trip to the moon would operate for a period on the order of 20 min. Therefore, higher radiator temperatures could be tolerated because of the shorter required operating time for gaseous nuclear rockets.

The third and last point to be made in comparing space radiators for gaseous nuclear rocket engines and electrical propulsion engines is that the maximum permissible temperature in a space radiator for an electrical propulsion engine must be less than the minimum temperature in the thermodynamic cycle employed to create the electric power. Such a limitation is not present for gaseous nuclear rockets. We can increase the temperature of the space radiator employed with a gaseous nuclear rocket engine as long as it can be tolerated by the materials.

Question: But this is something like 30,000 MW?

Answer: Yes. However, this would provide a method of developing a gaseous nuclear rocket engine using water as the propellant and then later on increasing the specific impulse of the engine by employing space radiators.

A second method of improving the specific impulse of a gaseous nuclear rocket engine developed using water as a propellant is illustrated on UAC Slide 29. Let us first examine the characteristics of an engine using entirely hydrogen as a propellant. The axial flow injected into the cavity is 1.0 lb/sec according to the example in UAC Slide 29. We saw in a preceding discussion that the resulting temperature of the flow injected into the cavity was extremely high. This flow injected into the cavity does not have enough heat capacity in getting to a cavity injection temperature of 5300 R to absorb all of the energy deposited in the moderator. A total of 5.0 lb/sec must be employed to remove the energy deposited in the moderator. Therefore, 4.0 lb/sec of the total flow must be injected downstream of the vortex tube as axial flow.

[redacted]

[redacted]

The flow rates required for a water rocket for the same power level shown in UAC Slide 29 are 4.3 lb/sec of axial flow within the cavity and 17.2 lb/sec of bypass flow for a total of 21.5 lb/sec of water flow. The reason for employing water in the cavity was to decrease the required density ratio and increase the fuel time constant. There is no reason to employ water as a moderator coolant other than to minimize the storage problem. Therefore, let us employ 4.3 lb/sec of water in the cavity and an additional 4.0 lb/sec of hydrogen as bypass flow to aid in cooling the moderator. The resultant total flow of 8.3 lb/sec would be brought to an average enthalpy of 120,000 Btu/lb and a resulting specific impulse of 2000 sec. Therefore, an engine developed using water as a propellant with a specific impulse of 1200 sec can be used to obtain 2000 sec by changing the moderator cooling fluid without the use of a space radiator. Similar improvements could be obtained in rockets which were developed using methane as a propellant.

In summarizing this portion of the discussion, we appear to have simulated the density ratios and time constants in our present tests which are required to obtain satisfactory performance from a water rocket. However, we do not have the correct simulation of Reynolds numbers.

A question was asked in a preceding discussion on methods of testing gaseous nuclear rocket engines. Pratt & Whitney Dependable Engines have been made dependable by an exhaustive test program to uncover difficulties. To get similar reliability from a gaseous nuclear rocket engine, we would have to test the engine without contaminating the atmosphere. One method of accomplishing this is illustrated in UAC Slide 30. A reference propellant flow of 1 lb/sec is employed in the discussion of UAC Slide 30. For this reference flow, approximately 2000 lb/sec of water coolant fluid would be required to reduce the temperature of the mixture to 170 F. The resulting exit flow would be 32 ft^3 of liquid water and 230 ft^3 of gaseous hydrogen. One method of avoiding the requirement of a large container for this hydrogen flow would be to inject 8 lb/sec of oxygen (a stoichiometric mixture with the hydrogen) and an additional 500 lb/sec of cooling water to provide the configuration shown in the second row of UAC Slide 30. For this configuration, 40 ft^3/sec of water would be generated for each pound per second of hydrogen propellant. Calculations indicate that all of the fission products would be soluble in the coolant water flow. The possibility of atmospheric contamination by evaporation of this water and the fission products could be minimized by covering the lower pond with a plastic film or by enclosing the lower pond.

Following a test, a pump would be used to raise the water from the

[redacted]

[redacted]

lower downstream pond to the upper upstream pond. This water would be pumped through a separator to recover unburned plutonium and fission products. Therefore, the upper pond would be relatively free of contamination.

In summary, it is obvious that we are very enthusiastic about the possible performance gains that could be obtained from gaseous nuclear rockets. However, we are not yet in a position to recommend a development program. We do believe that the theoretical and experimental results which we have obtained are sufficiently encouraging to recommend that gaseous nuclear rocket research programs be pursued more vigorously. Hopefully, such a vigorous program conducted over a period of several years would lead to the possibility of recommending a true development program. However, I repeat that we do not yet recommend a development program. That concludes our presentation. Are there any questions?

Question: What is the basis for the 10^{-3} separation ratio?

Answer: Ralph Cooper specifically omitted discussions of economics in this symposium. About all we can say is that it is a desirable economic goal.

Question: What makes you think you can get a separation ratio of 10^{-3}?

Answer: Extrapolation of our containment measurements to higher Reynolds numbers.

Question: Your tests were conducted without radiant heat transfer?

Answer: Yes, but radiant heat transfer should give us a radial temperature gradient which should be stabilizing. That is, the difference in density of the hot fluid in the center relative to the cold fluid in the outside should help suppress turbulence.

Question: Do you have any verification of the R^2 dependence of this dimensionless time constant?

Answer: We have conducted tests in water vortex tubes having diameters of both 4 and 10 in. The time constant in the smaller tube was on the order of 10 min, while in the larger tube it was on the order of 1 hr. This ratio of time constant is approximately equal to the ratio of the square of the tube radii. In addition, there is theoretical justification for believing that the time constant should vary as the square of the tube radius.

Question: What is the pressure shell made of?

Answer: We are not sure. The weight estimates which we have employed assumed steel with a strength of 200,000 psi. This assumed stress limit is considerably lower than the stresses envisioned from chemical rocket engine

[redacted]

cases. The weight would probably come down further by the use of filament-wound construction.

Question: What is the relative heat deposition rate at the inside edge of the moderator in the pressure shell?

Answer: The heat deposition rate at the inside edge of the moderator is on the order of 10^5 Btu/sec-ft^3. The heat deposition rate in the pressure shell would be two or more orders of magnitude less than this figure.

Question: Is the 10 atm pressure drop for moderator cooling flow an upper limit?

Answer: No, this pressure drop varies very rapidly with void volume fraction and the diameter of the coolant passage ducts.

Question: How valid are your scaling parameters?

Answer: We have no reason to doubt these scaling parameters now and hope to verify them at different Reynolds numbers in the future. It is undoubtedly cheaper to verify these parameters to the best of our ability with cold flow before going to an actual rocket engine. However, eventually full-scale tests would be required if the assumption is made that everything continues to show promise in this concept.

Question: Do you have any hopes of simulating the temperature characteristics you have to have in order to get the thermal radiation?

Answer: The power required is extremely high. We hope to get verification of some of the radiant heat transfer work by shock tube tests.

Question: The flow rate of hydrogen that you mentioned in your last slide was approximately 0.1% of the flow in a full-scale engine. Can this be scaled?

Answer: Yes, the numbers shown on UAC Slide 30 were for a reference propellant flow of 1 lb/sec. All flow quantities shown in this slide should be multiplied by the actual propellant flow. For instance, a flow of 1000 lb/sec of propellant for a period of 1 min would result in a total water usage of 1.2×10^8 lb of water. This would fill a pond 50 ft deep having an area of 1 acre. A preliminary estimate of the cost of such ponds and the required separator and pump facilities indicates a cost on the order of several million dollars, exclusive of the test stand itself.

Question: Are you saying that you think you could test a full-scale engine underground?

Answer: Yes, the required size of the pond depends on the size of the engine and the length of the tests.

[redacted]

Question: What about delay neutrons?

Answer: If the fuel stayed in for 12 sec, the source of delay neutrons would also stay in for 12 sec. Therefore, you would retain some of the controllability of the engine which comes from the delay neutrons.

Question: What about startup?

Answer: Our preliminary studies have indicated that a chemically powered turbine might be employed to start the hydrogen pumps. Once the flow is established, uranium-hexafluoride might be put in the cavity to make it critical. As soon as power was being generated, the energy deposited in the wall could be used in the regular turbopump cycle. Once the temperature of the gases in the cavity exceeded a certain amount, further fuel feed might be accomplished by injecting solid pellets of plutonium.

Question: Aren't these pellets accelerated and thrown out of the vortex as fast as they are injected?

Answer: It only requires on the order of 0.001 sec for the pellets to evaporate once they get into the high-temperature region.

Comment: We're thinking of hollow spheres for this reason.

Question: What is the relative fuel temperature for a hydrogen rocket and a water rocket?

Answer: Because dissociated water is two-thirds hydrogen, we have assumed that the opacities of water are equal to those of hydrogen, and that the resulting temperature distributions for water and hydrogen rockets are identical.

Question: Isn't the propellant temperature using water higher than the propellant temperature using hydrogen?

Answer: Yes, but the temperature of the propellant in the cavity tends to be much higher than the temperature corresponding to a hydrogen specific impulse of 2500 sec. The hydrogen at the temperatures in the propellant region has an enthalpy which corresponds to a specific impulse on the order of 6000 sec. This same temperature corresponds to a specific impulse of 2500 to 3000 sec with water.

Question: Is that the average temperature of the propellant in the chamber?

Answer: Yes.

Question: What about dissociation of water and hydrogen?

Answer: We have included this effect. For instance, water at high temperatures consists of hydrogen atoms, hydrogen ions, singly-ionized oxygen

[redacted]

atoms, doubly-ionized oxygen atoms, triply-ionized oxygen atoms, and electrons.

Question: I don't understand why the specific impulse isn't 6000 sec for hydrogen.

Answer: Since 10% of the energy is deposited in the wall, we either have to use a large amount of additional hydrogen coolant to remove this energy, or we have to employ a space radiator. The specific impulse with a space radiator using hydrogen propellant could be on the order of 6000 sec. However, the specific impulse for an engine not employing a space radiator would be limited to something like 2500 sec with hydrogen propellant.

Question: What about nozzle recombination?

Answer: Our assumed nozzle efficiency of 80% is designed to take into account any inefficiencies due to delays in nozzle recombination. However, it does not look like nozzle recombination should be a problem.

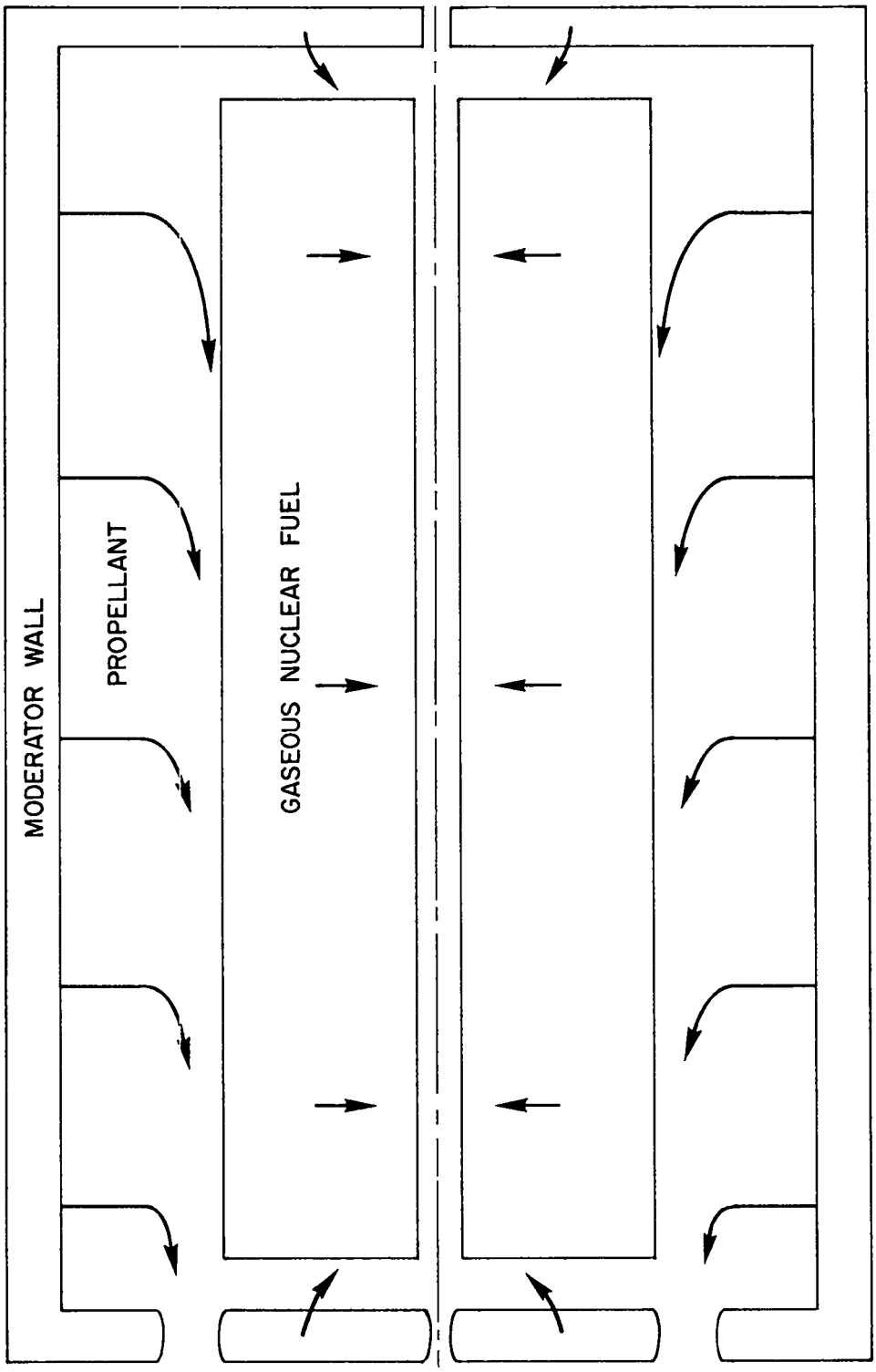

Slide 1

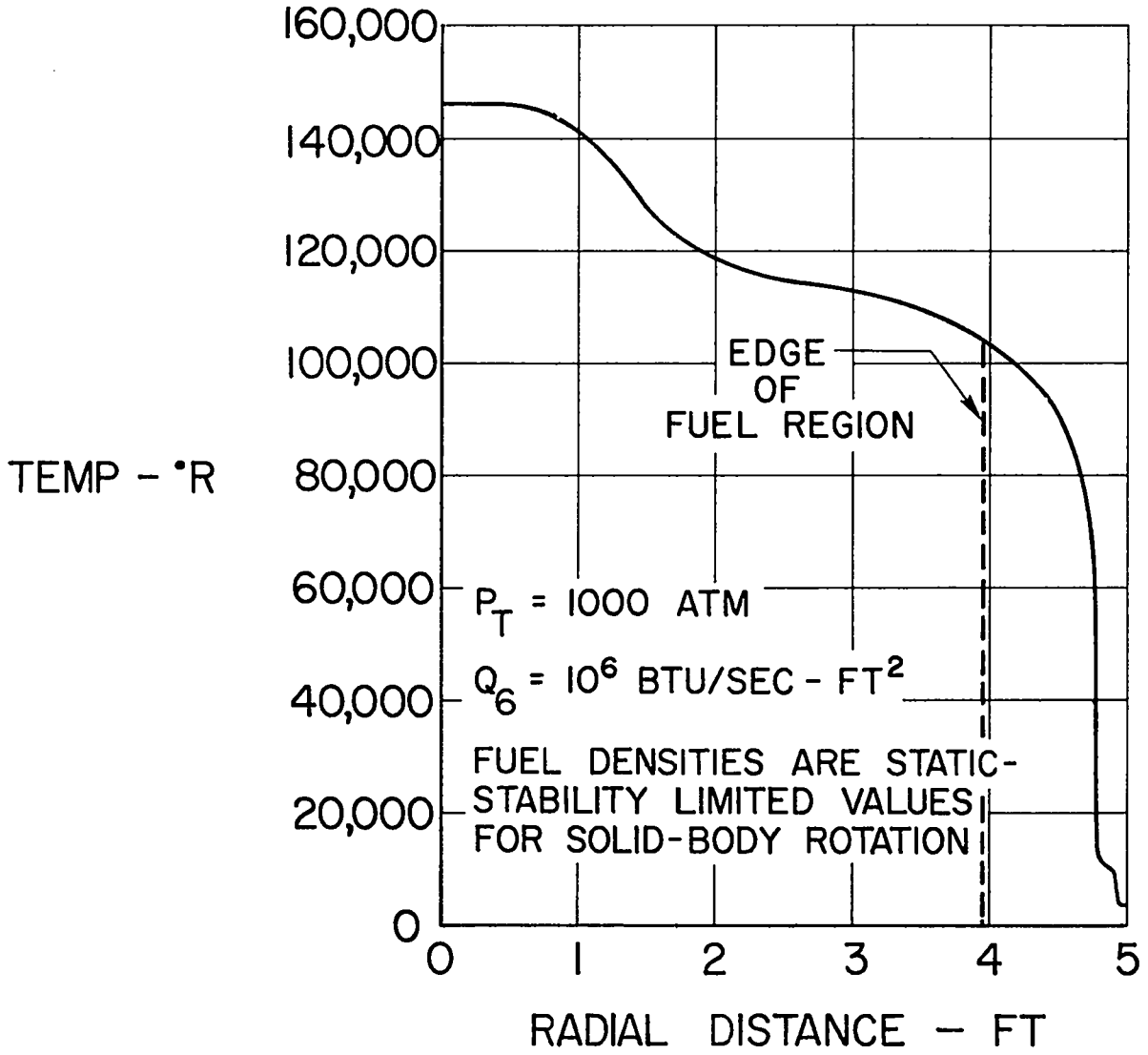

Slide 2

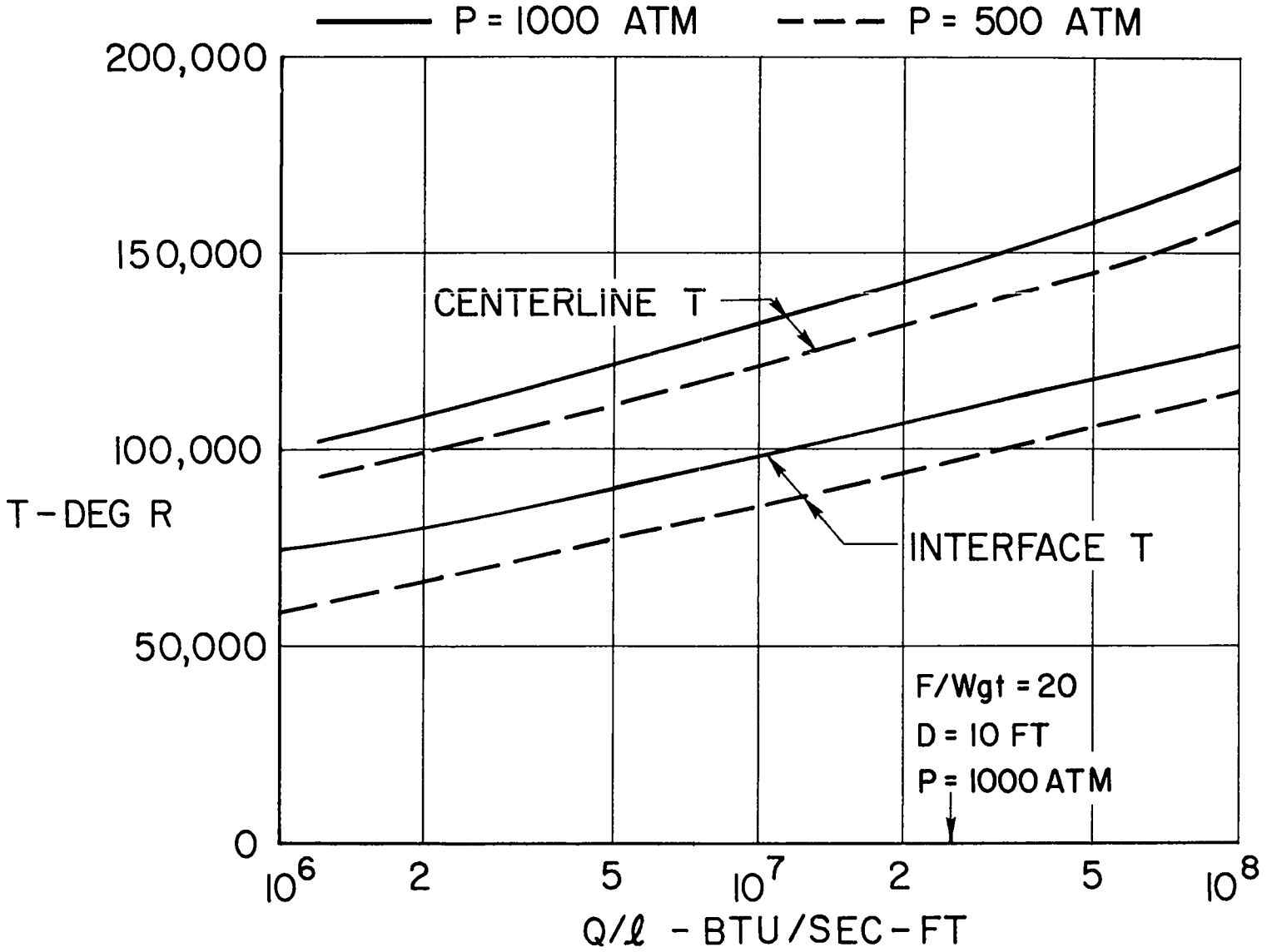

Slide 3

APPROVED FOR PUBLIC RELEASE

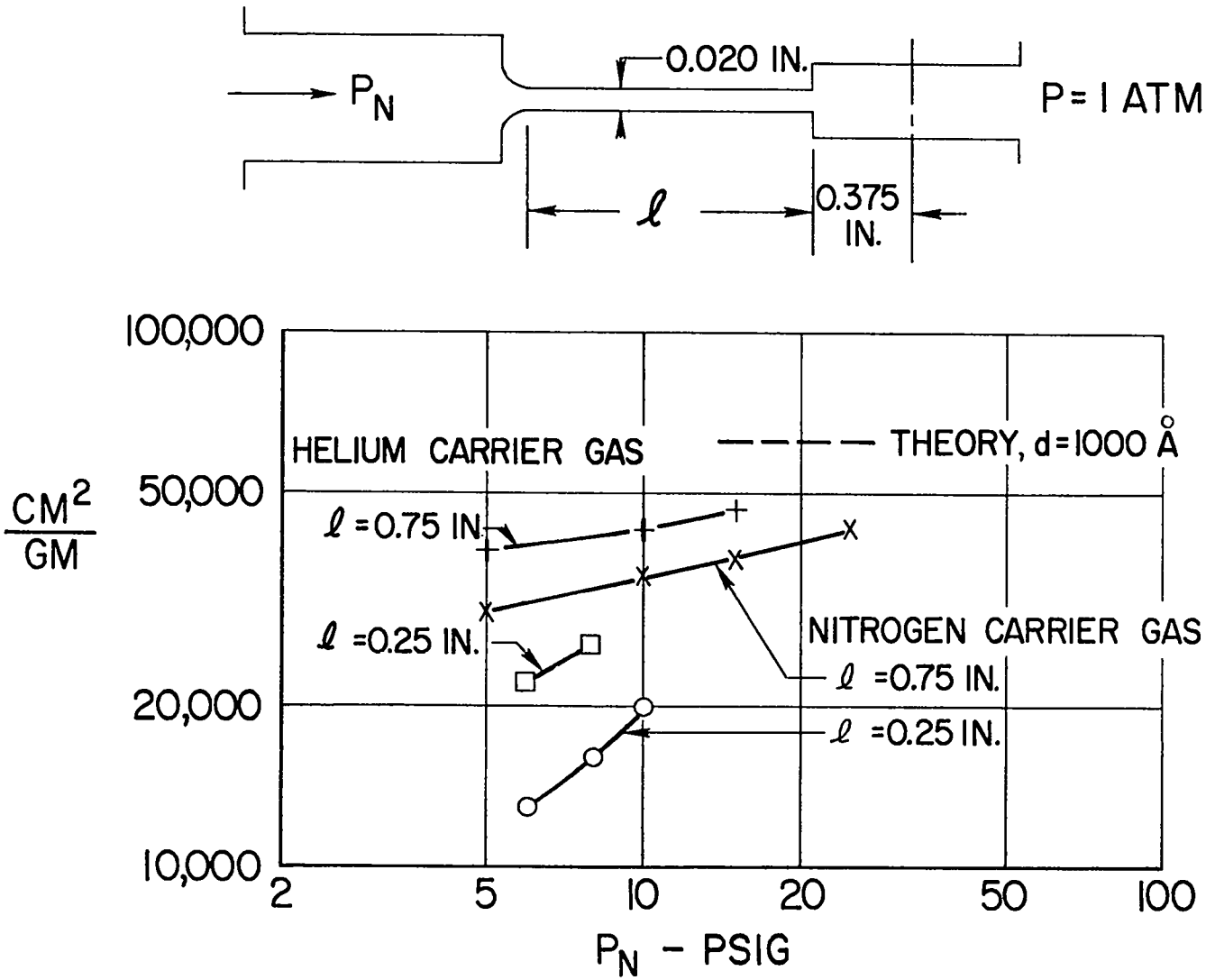

Slide 4

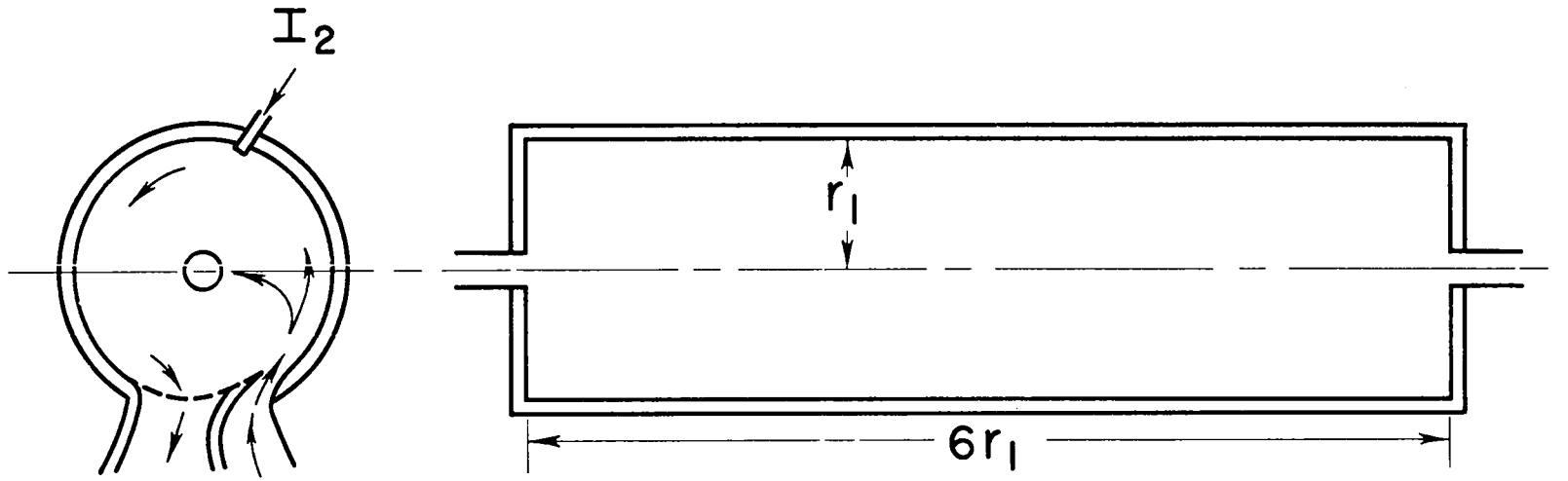

BASIC VORTEX TUBE

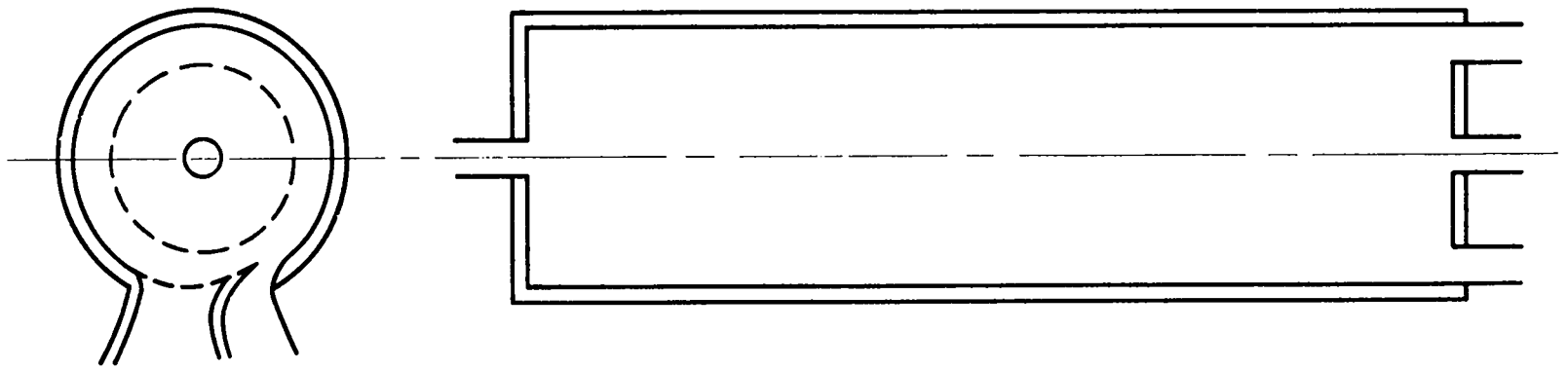

AXIAL-FLOW VORTEX TUBE

Slide 5

APPROVED FOR PUBLIC RELEASE

[redacted]

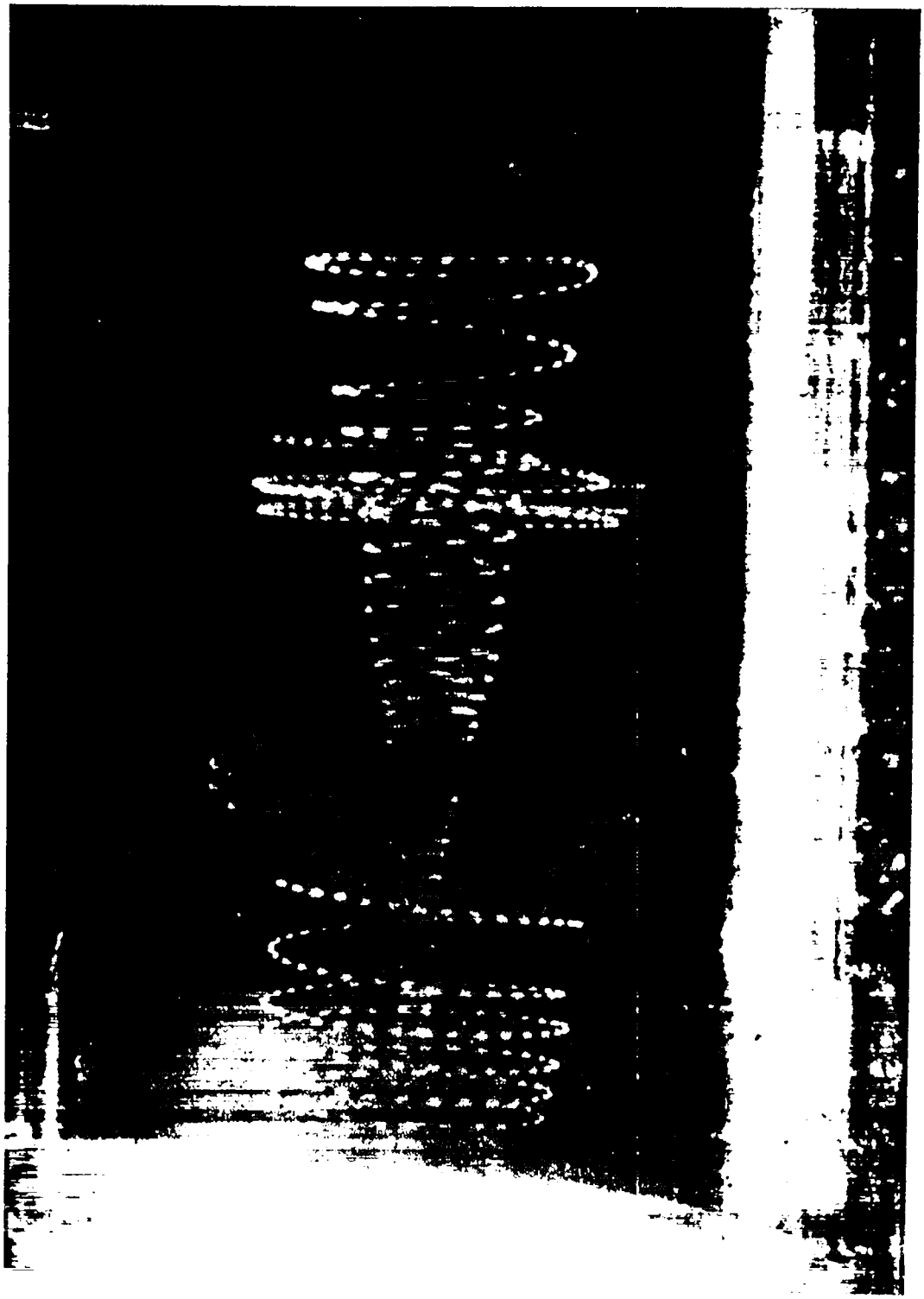

Slide 6

[redacted]

[redacted]

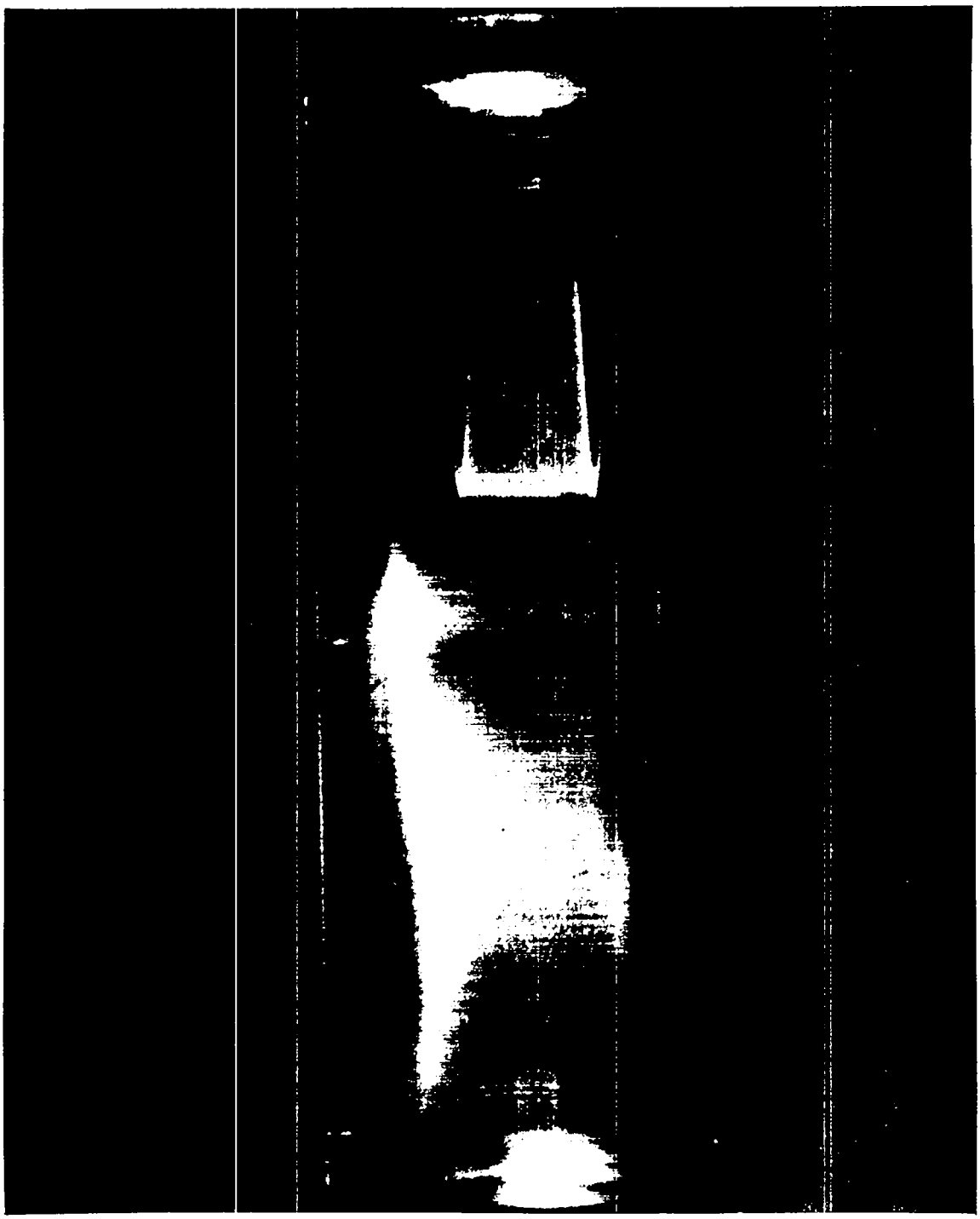

Slide 7

[redacted]

[redacted]

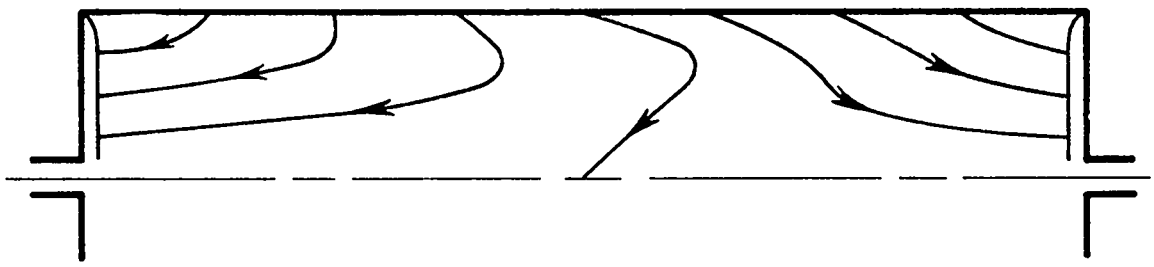

LARGE THROUGH-FLOW RATE

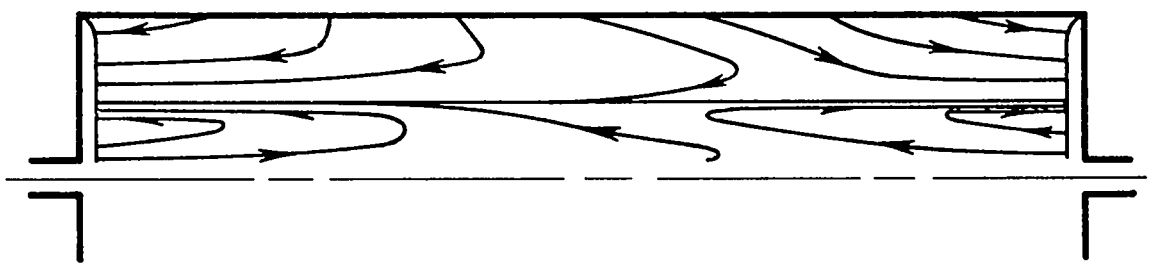

SMALL THROUGH-FLOW RATE

Slide 8

[redacted]

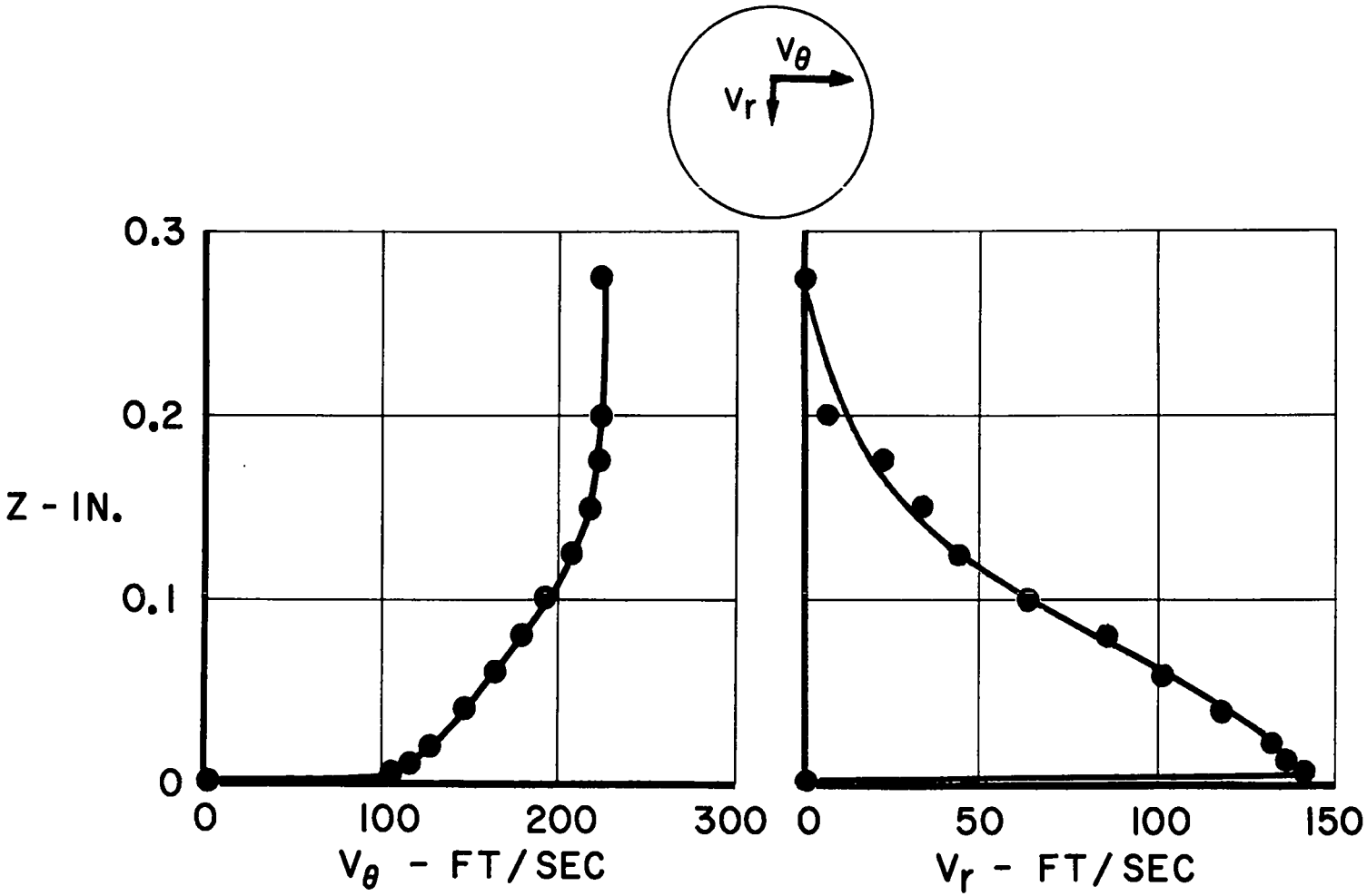

Slide 9

APPROVED FOR PUBLIC RELEASE

[redacted]

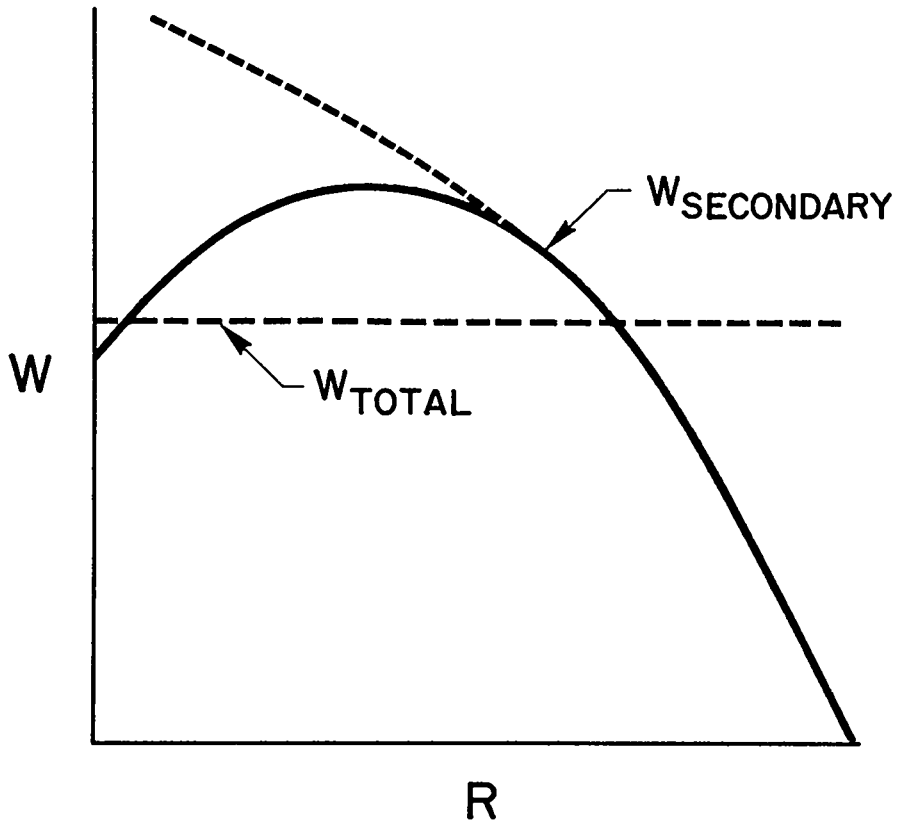

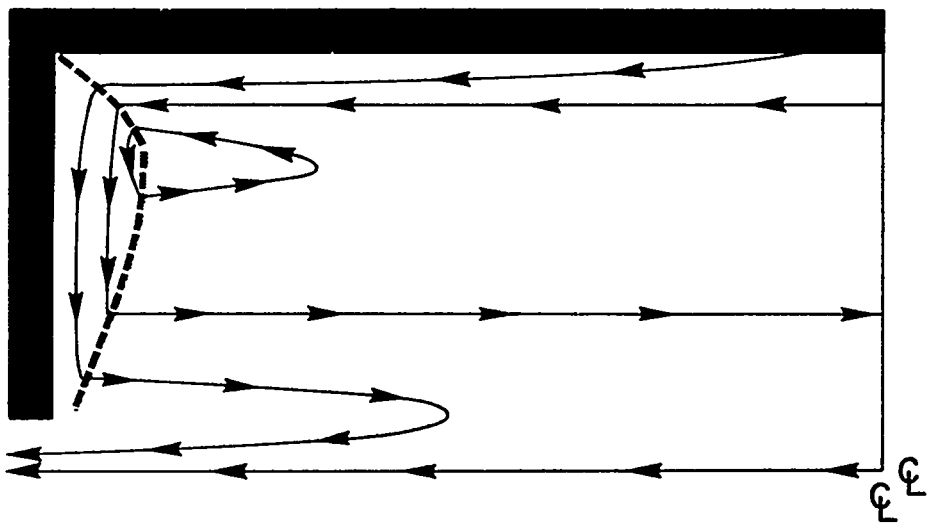

Slide 10

[redacted]

[redacted]

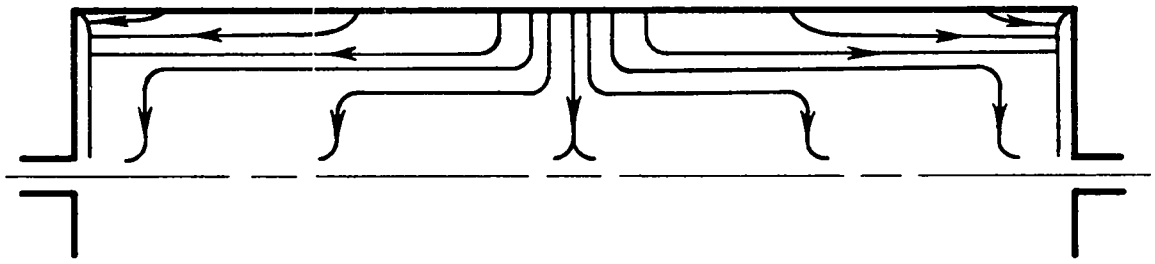

SMALL THROUGH-FLOW RATE
WITH END-WALL SUCTION

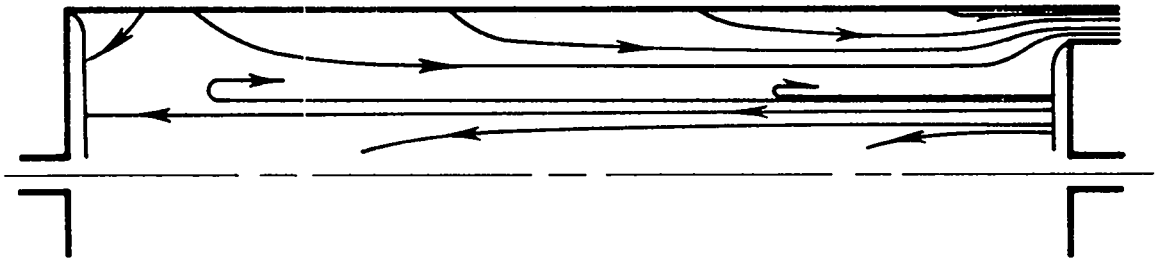

SMALL THROUGH-FLOW RATE
WITH AXIAL FLOW

Slide 11

[redacted]

[redacted]

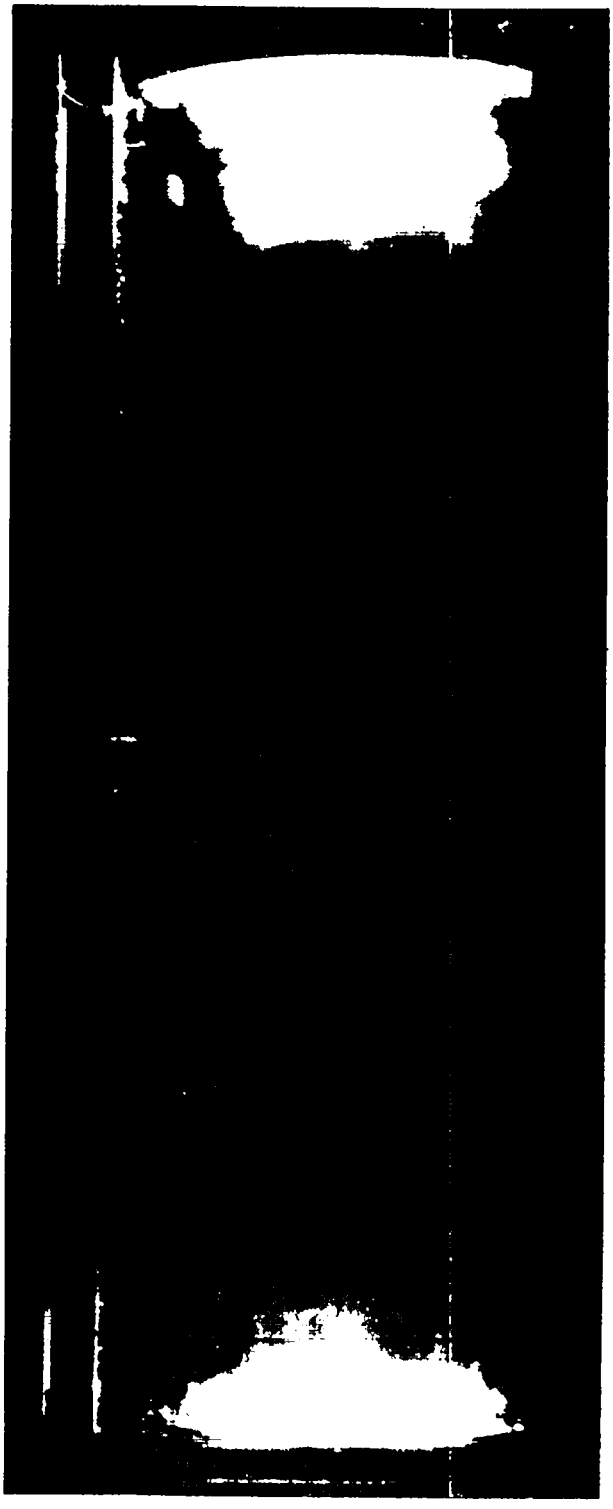

Slide 12

[redacted]

[redacted]

Slide 13

[redacted]

[redacted]

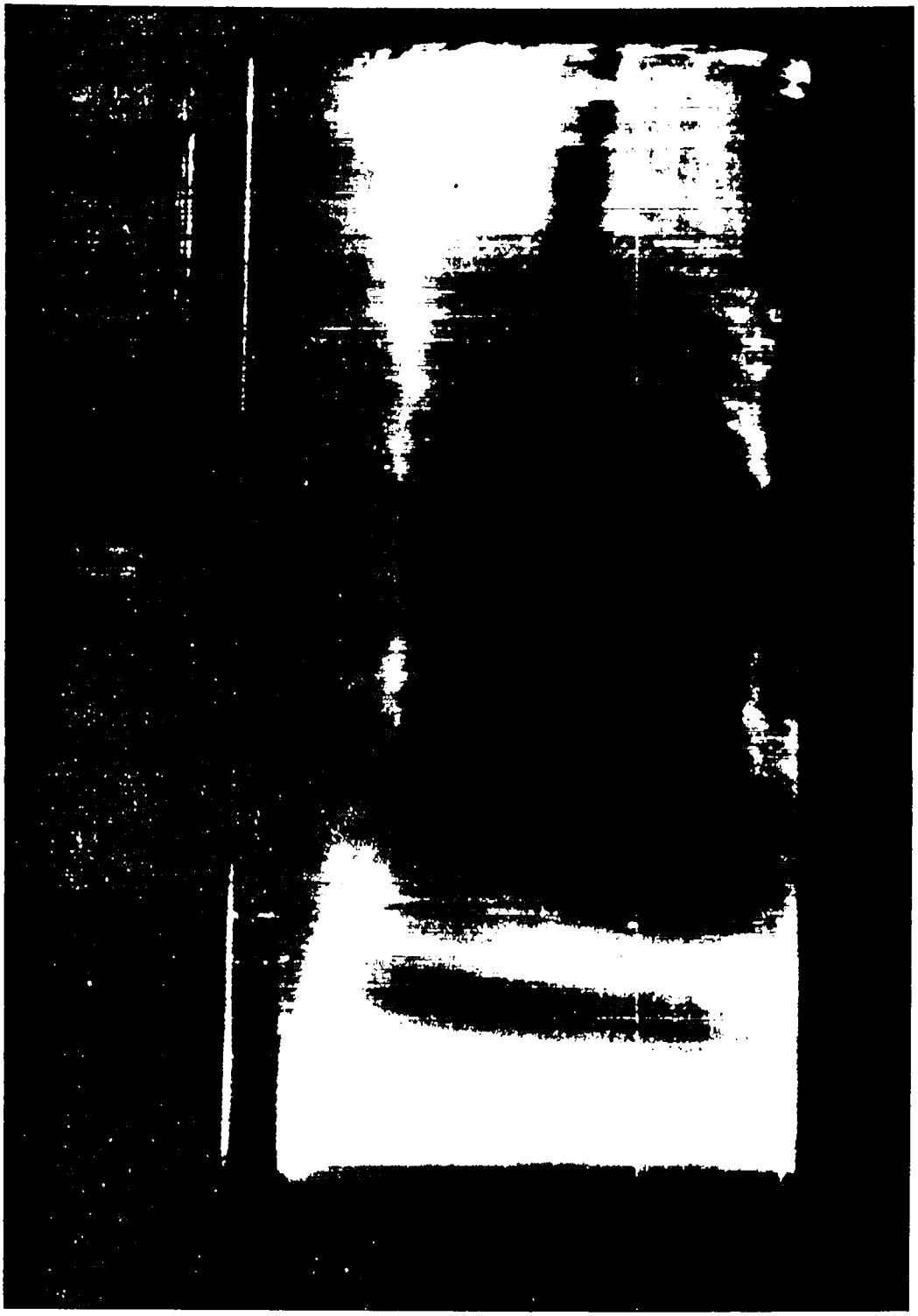

Slide 14

[redacted]

[redacted]

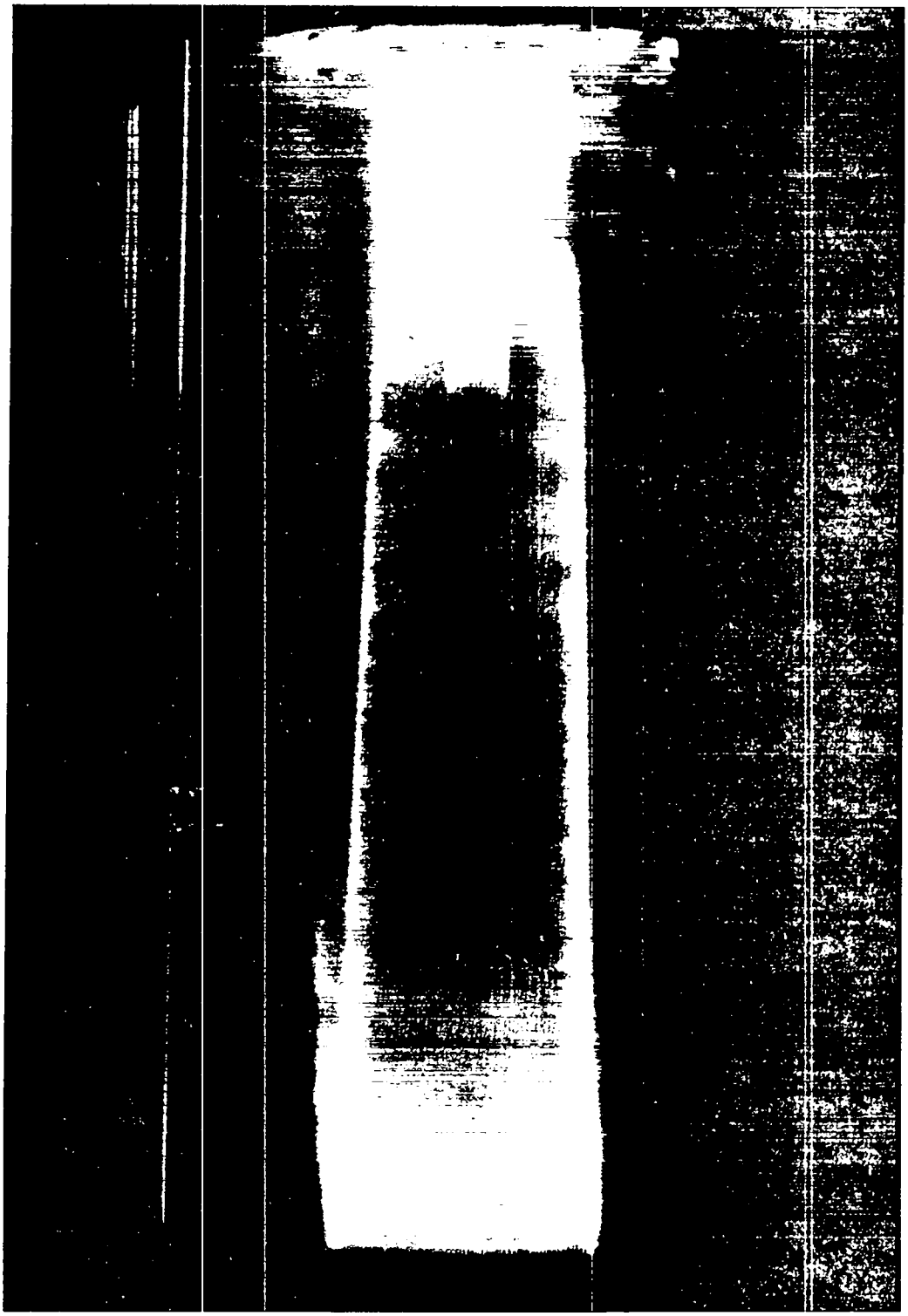

Slide 15

[redacted]

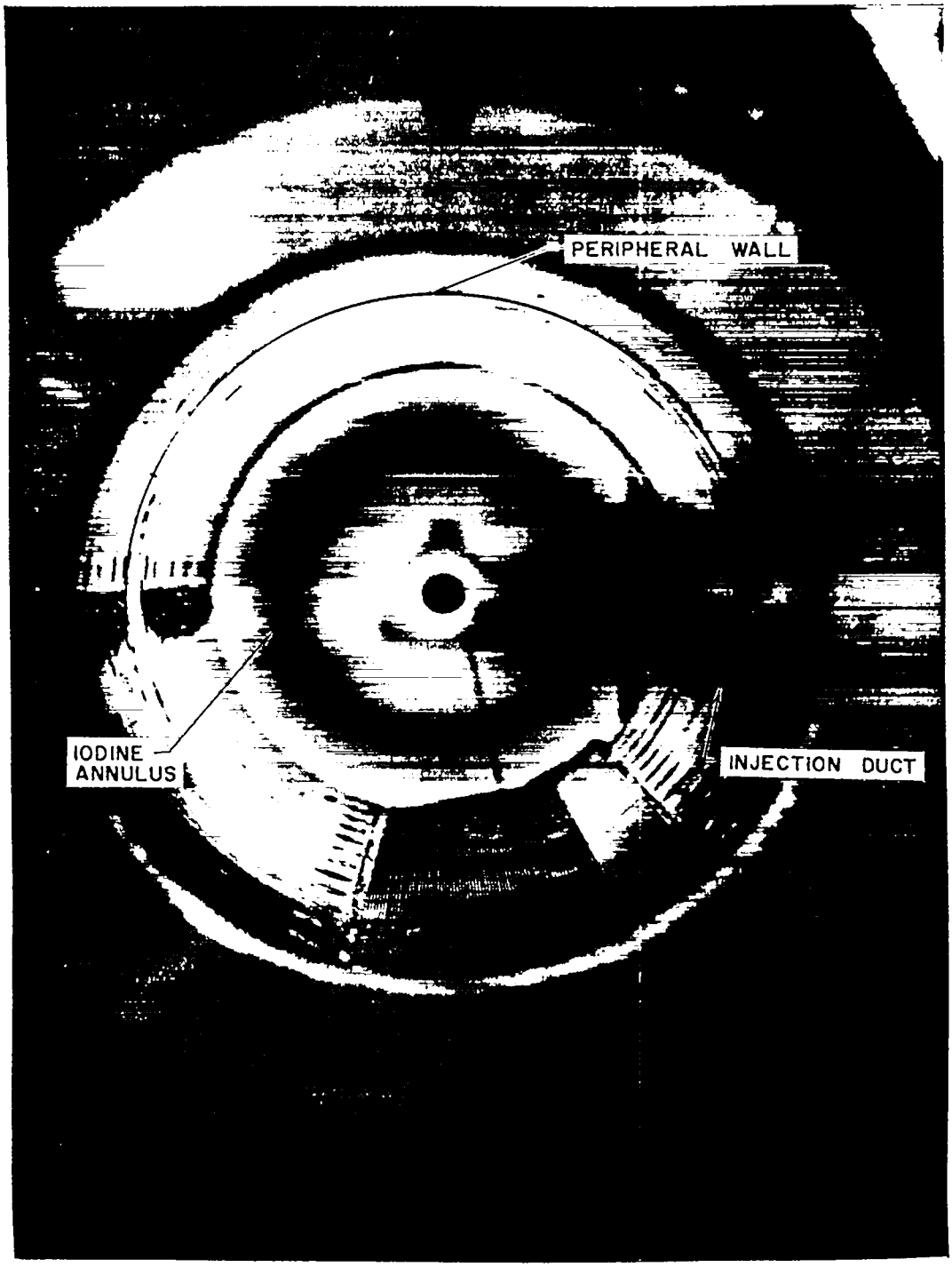

Slide 16

FLUIDS	$t = \frac{LB}{LB/SEC} = SEC$	$\frac{\rho r_1^2}{\mu} - SEC$	$\frac{t}{(\rho r_1^2/\mu)}$
I_2, He	0.5 TO 1.5	60	0.01 TO 0.03
I_2, AIR	4 TO 12	500	0.01 TO 0.03
DYE, H_2O	1000 TO 4000 *	16,000	0.06 TO 0.25 *

* - VISIBLE TIME

Slide 17

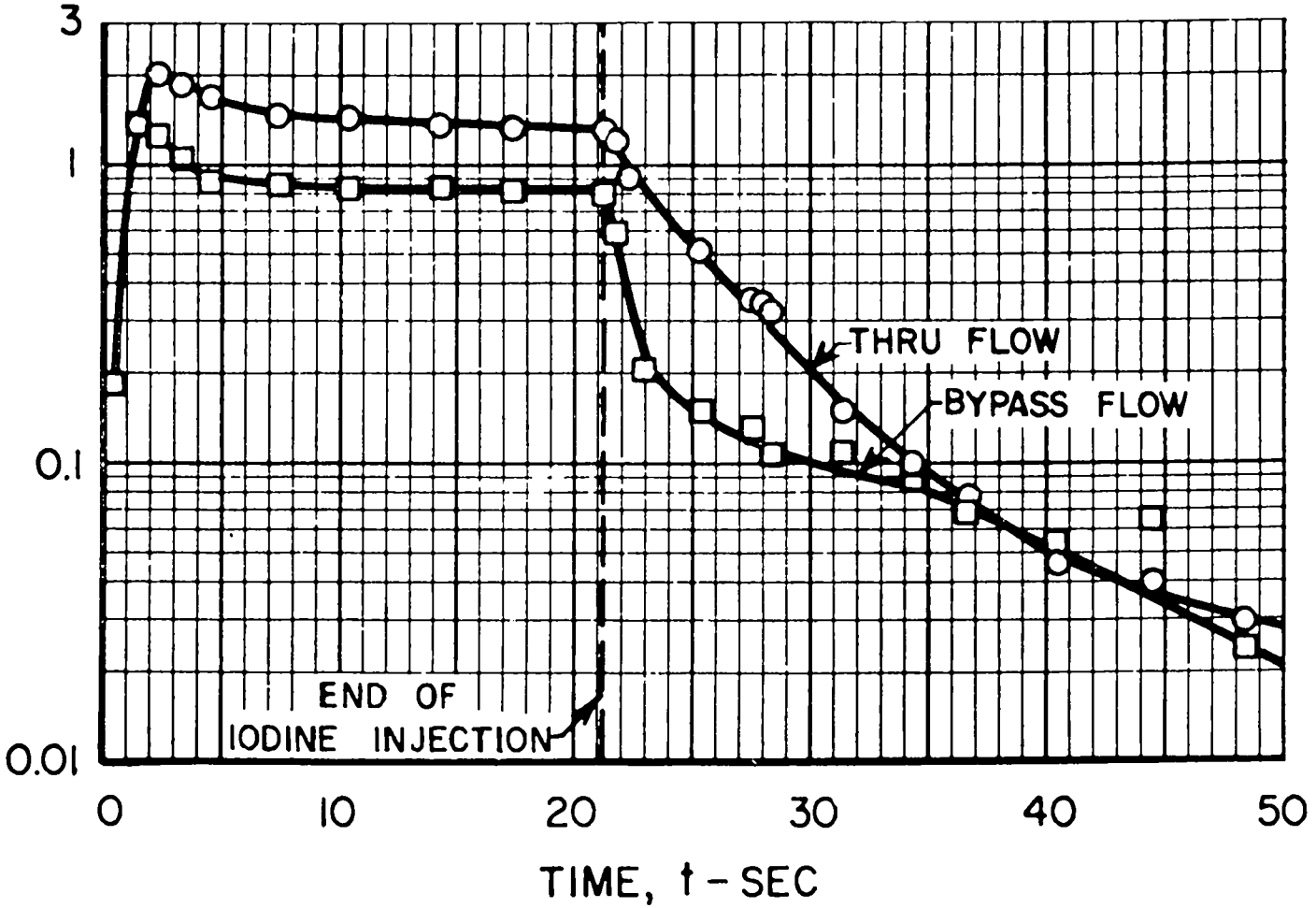

Slide 18

APPROVED FOR PUBLIC RELEASE

SYMBOL	HEAVY GAS	LIGHT GAS	END WALLS
○	IODINE	AIR	PLAIN
⌀	IODINE + FREON		
■	IODINE + FREON	HELIUM	PLAIN
▲	IODINE	HELIUM	DISTRIBUTED - FRICTION
◢	IODINE + FREON		

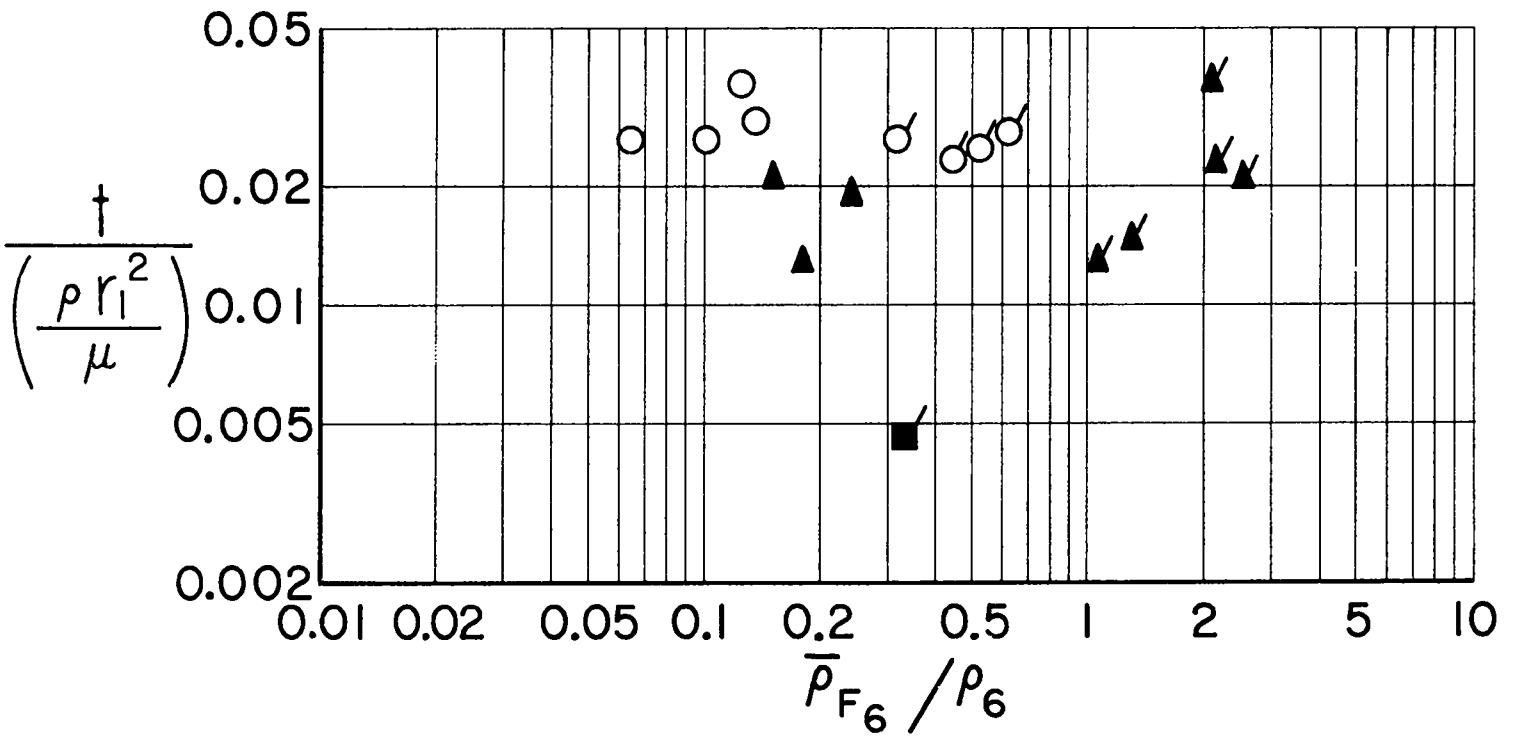

Slide 19

$$\frac{\tau}{\left(\frac{\rho r_1^2}{\mu}\right)}$$

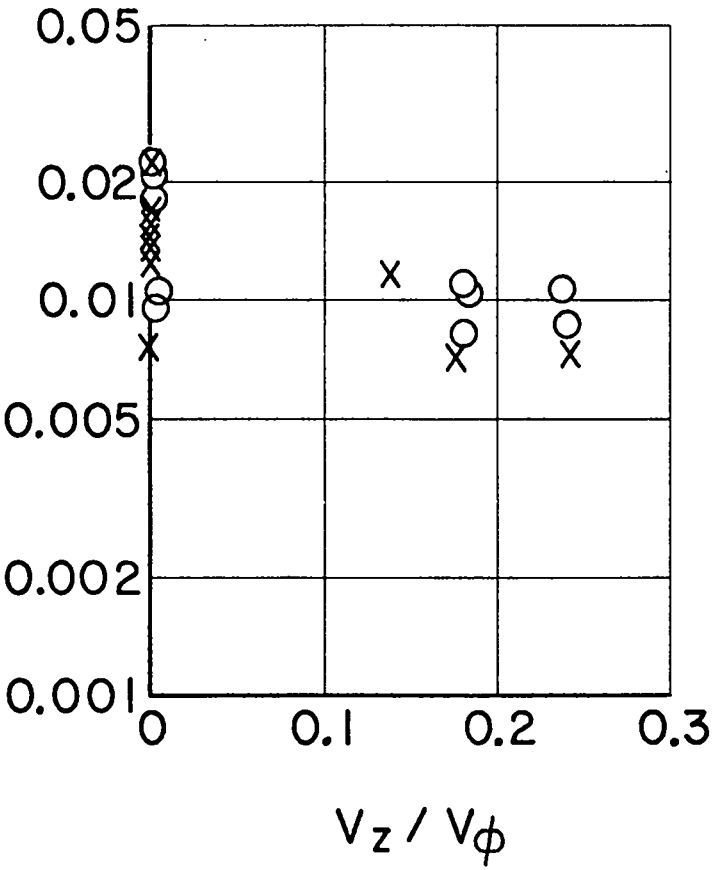

I_2 - AIR

o - Re_t = 40,000

x - Re_t = 70,000

$$Re_Z = \frac{V_Z}{V_\phi} Re_t$$

Slide 20

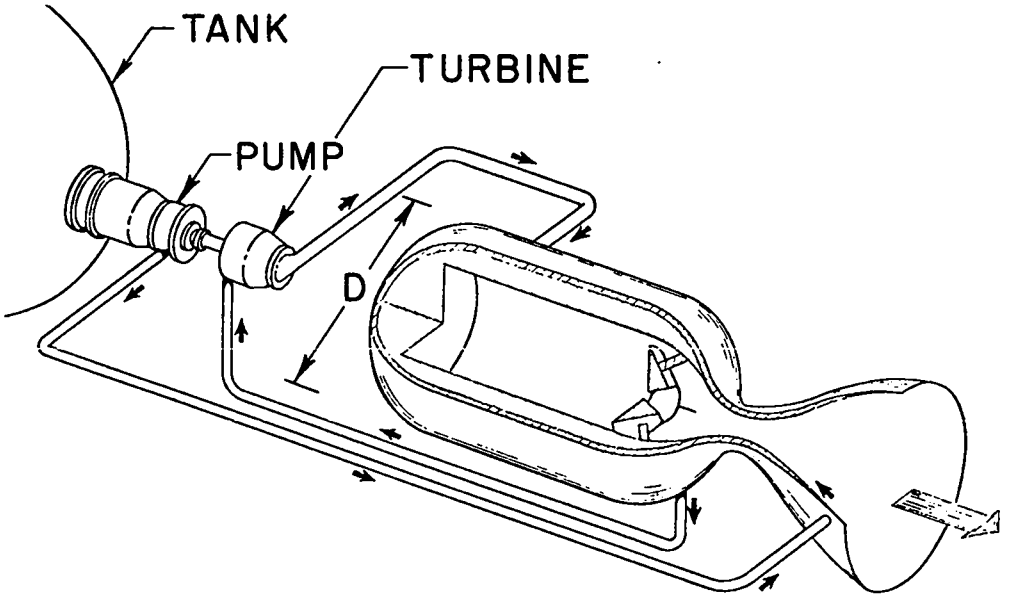

FOR D = 10 FT, P = 1000 ATM

$Wgt = 170{,}000$ LB

$W_H = 1350$ LB/SEC

$I_{sp} = 2500$ SEC

$F = 3{,}400{,}000$ LB

POWER = 285,000 MW

$\mathcal{W}_F = 7.5$ KG $= 16.5$ LB

$\overline{\rho}_{F_1} = 0.035$ LB/FT^3

$\overline{\rho}_{F_6} = 0.062$ LB/FT^3

$(W_F)_{1000} = 1.35$ LB/SEC

$$(t_f)_{1000} = \frac{16.5 \text{ LB}}{1.35 \text{ LB/SEC}} = 12 \text{ SEC}$$

Slide 21

APPROVED FOR PUBLIC RELEASE

DENSITY RATIO REQUIREMENTS

$D = 10$ FT

$\bar{\rho}_{F_6} = 0.062$ LB/FT^3

$F = 3.4 \times 10^6$ LB

$F/Wgt = 20$

$I_{sp} = 2500$ SEC

$P = 1000$ ATM

PROPELLANT	ρ_6 - LB/FT^3	$\bar{\rho}_{F_6}/\rho_6$
H_2	0.0065	9.5
CH_4	0.020	3.2
NH_3	0.026	2.4
H_2O	0.035	1.7

$\frac{\bar{\rho}_F}{\rho_6}$ IN MODEL TESTS = 0 $\longrightarrow$ 2.2

Slide 22

APPROVED FOR PUBLIC RELEASE

F/Wgt = 20 —— P = 1000 ATM

I_{sp} = 2500 SEC - - - P = 500 ATM

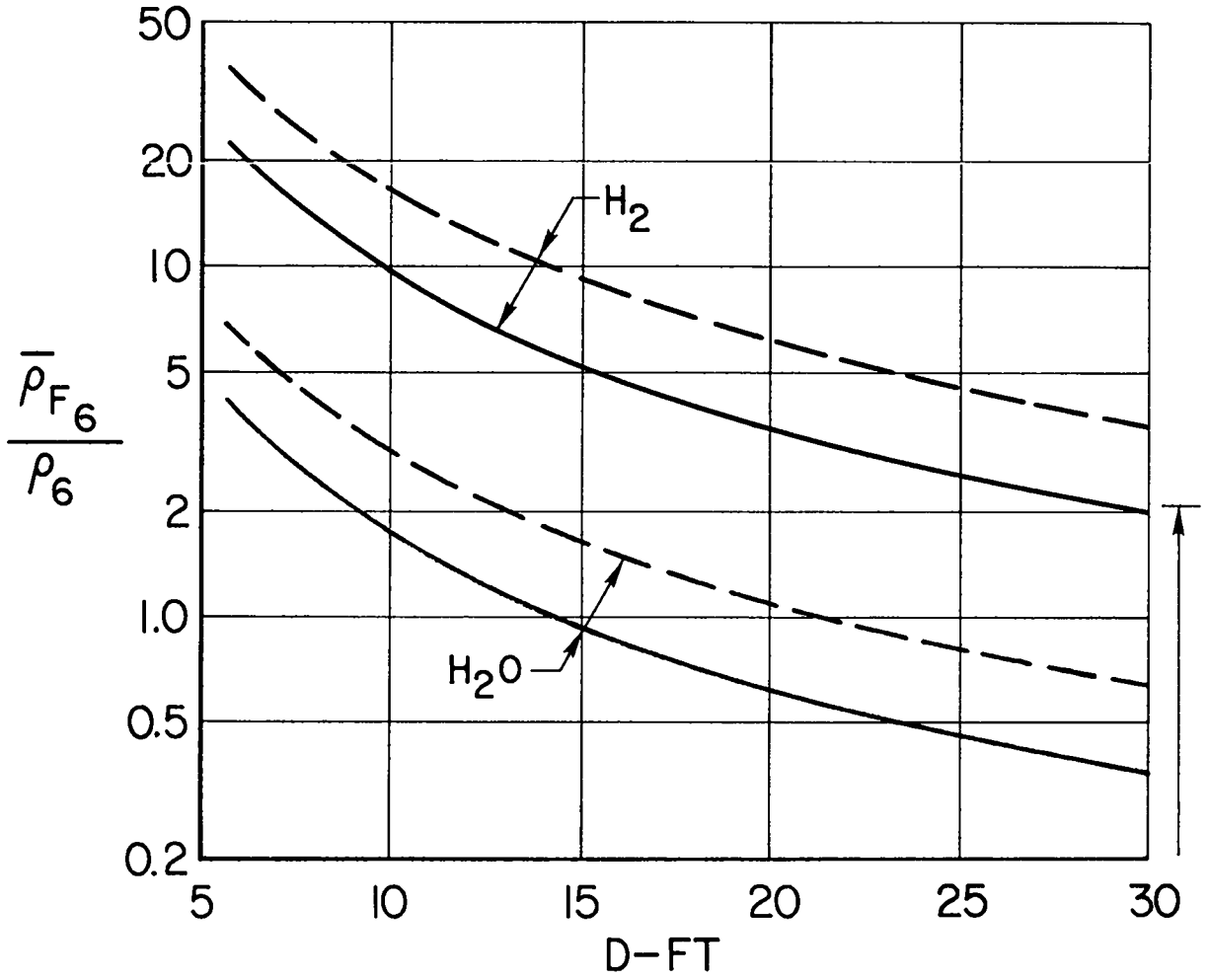

Slide 23

TIME CONSTANT REQUIREMENTS

D = 10 FT

$F = 3.4 \times 10^6$ LB

F/Wgt = 20

I_{sp} = 2500 SEC

P = 1000 ATM

$$(t_f)_{1000} = \frac{16.5 \text{ LB}}{1.35 \text{ LB/SEC}} = 12 \text{ SEC}$$

PROPELLANT	$\left(\frac{\rho r_1^2}{\mu}\right)$ - SEC	$\tau_{f_{1000}} = 12 \text{ SEC} \Big/ \left(\frac{\rho r_1^2}{\mu}\right)$
H_2	214	0.056
CH_4	632	0.019
NH_3	857	0.014
H_2O	1200	0.010

τ_f MEASURED IN MODEL TESTS = 0.005 → 0.030

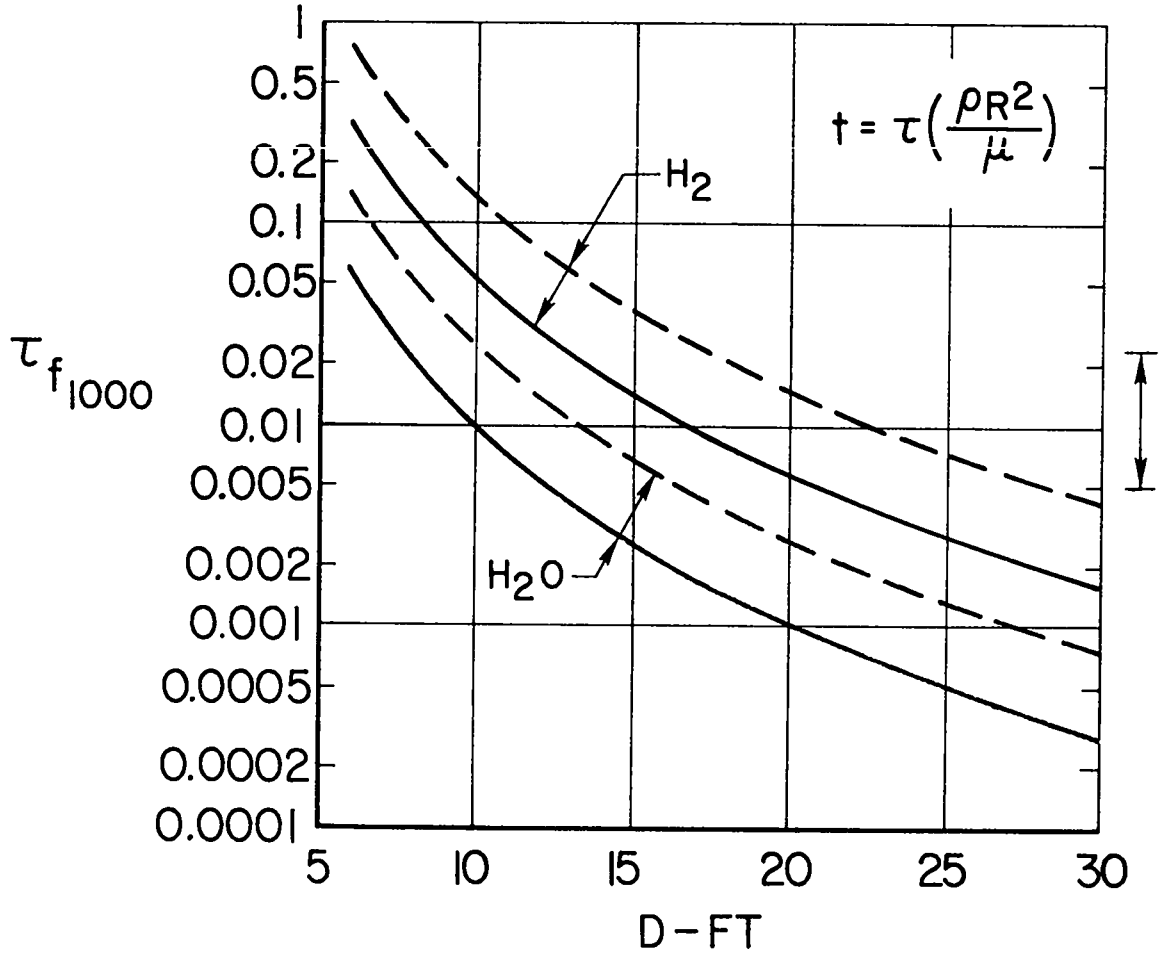

Slide 25

APPROVED FOR PUBLIC RELEASE

$$Re_z = \frac{\rho_4 V_{z_e} r_1}{\mu_4}$$

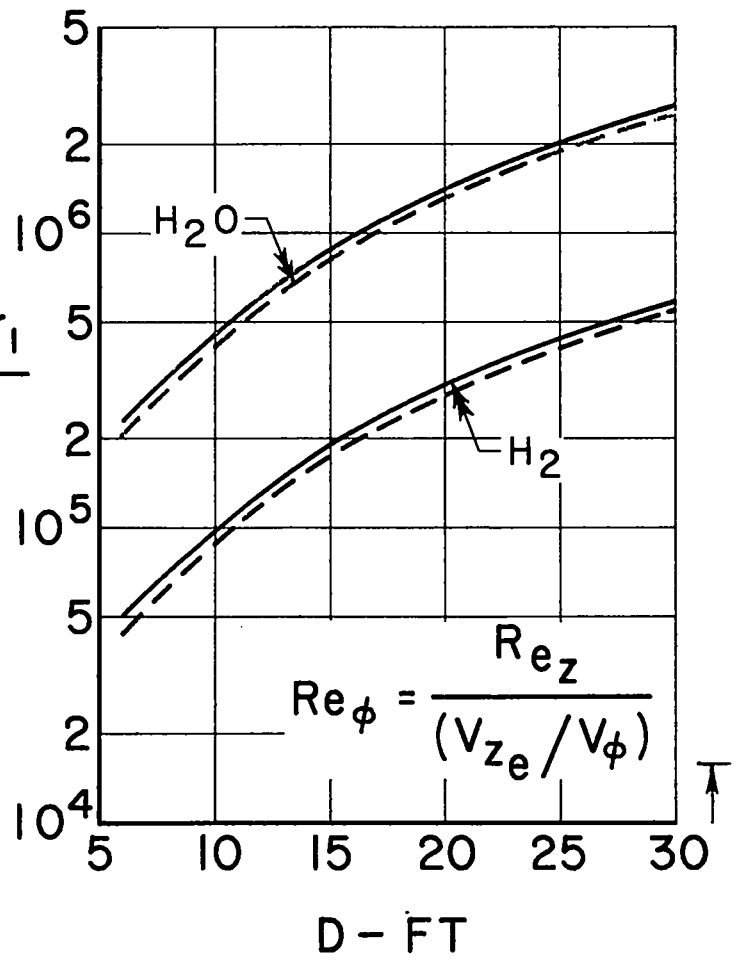

F/Wgt = 20

I_{sp} = 2500 SEC

—— P=1000 ATM

— — P=500 ATM

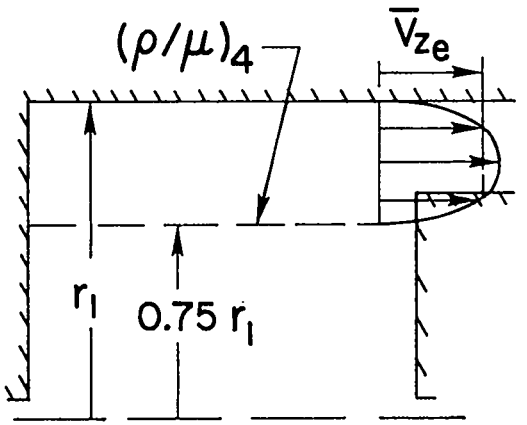

Slide 26

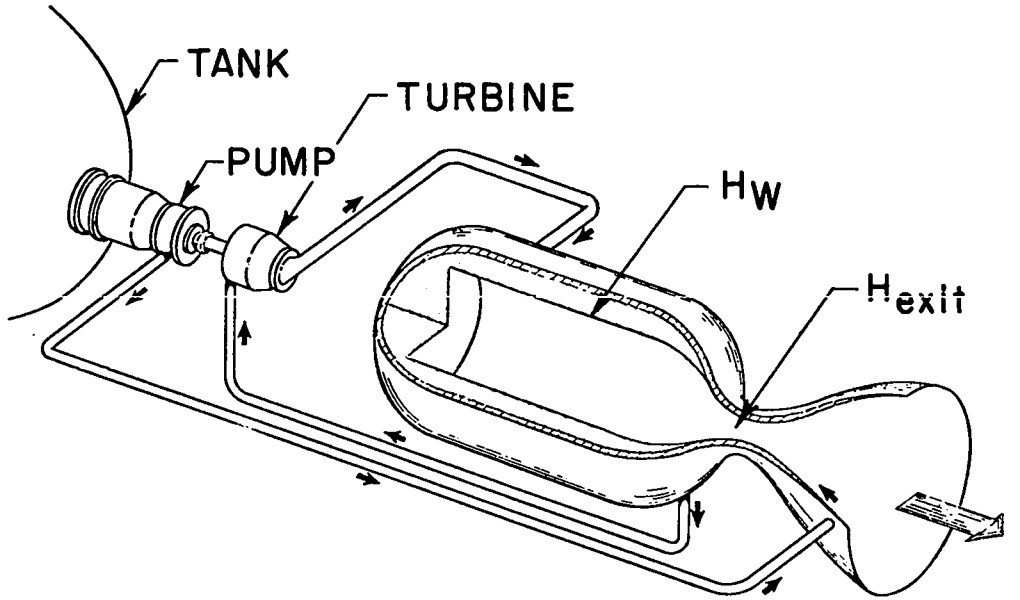

PROPELLANT	H_W at T = 5300 R BTU/LB	$H_{exit} = 10\ H_W$ BTU/LB	I_{sp} = SEC
H_2	20,000	200,000	2500
CH_4	10,000	100,000	1800
NH_3	6700	67,000	1450
H_2O	4600	46,000	1200

Slide 27

APPROVED FOR PUBLIC RELEASE

T_{RAD}, °R	Wgt		
	$\frac{LB}{FT^2}$	$\frac{LB}{BTU/SEC}$	LB/KW
2000	1.0	0.130	0.123
4000	1.0	0.00813	0.00772
6000	1.0	0.00161	0.00153

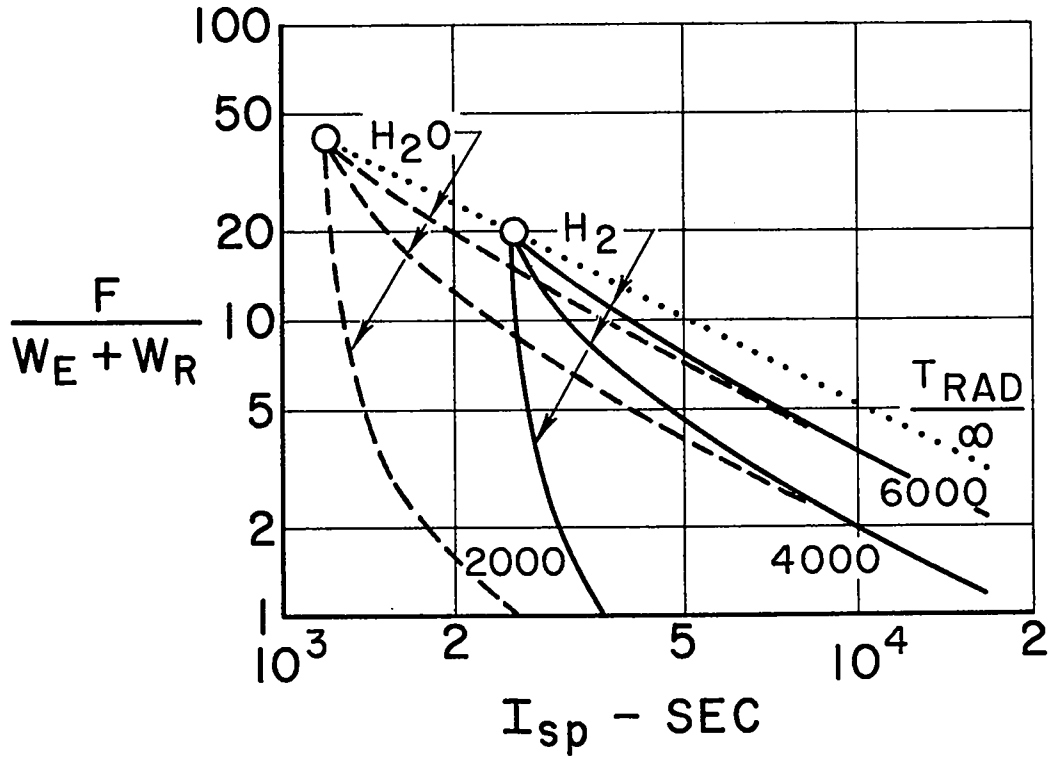

Slide 28

APPROVED FOR PUBLIC RELEASE

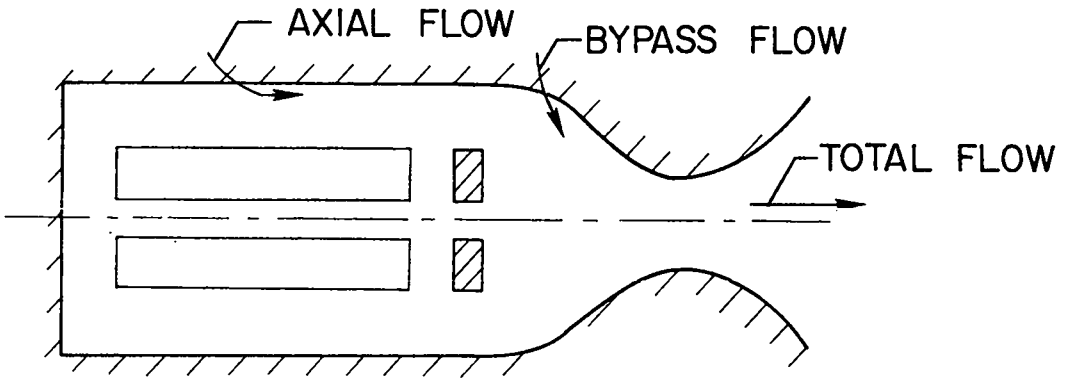

$q_T = 10^6$ BTU/SEC $\quad q_W = 10^5$ BTU/SEC

		FLUID	FLOW - LB/SEC	$\bar{H}$ - BTU/LB	I_{sp} - SEC
I	AXIAL BYPASS	H_2 H_2	1.0 4.0	200,000	2500
II	AXIAL BYPASS	H_2O H_2O	4.3 17.2	46,000	1200
III	AXIAL BYPASS	H_2O H_2	4.3 4.0	120,000	2000

Slide 29

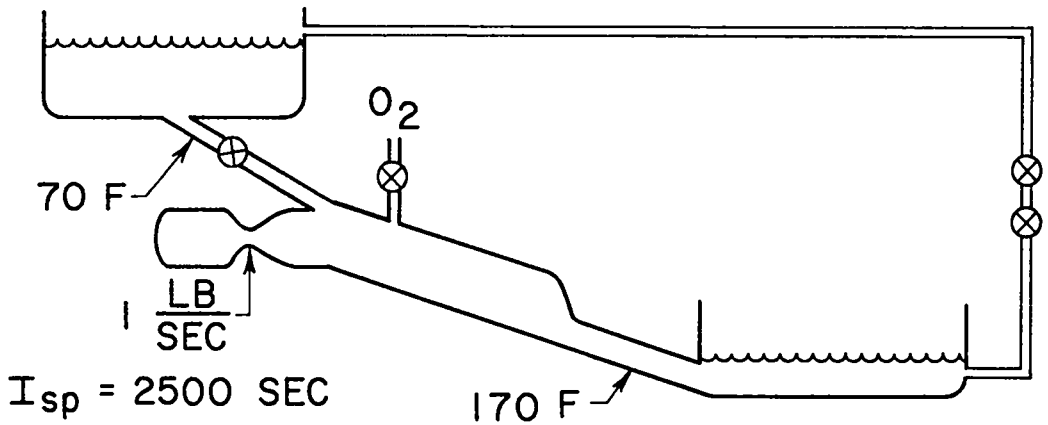

	INLET FLOW LB/SEC		EXIT FLOW FT^3/SEC	
	O_2	H_2O	LIQUID	GAS
H_2	0	2000	32	230
	8	2500	40	0
CH_4	0	2000	32	29
NH_3	0	2000	32	0
H_2O	0	2000	32	0

Slide 30

APPROVED FOR PUBLIC RELEASE

[redacted]

HELIOS

Theodore F. Stubbs
Lawrence Radiation Laboratory
Livermore, California

As was mentioned, the HELIOS concept is by no means new. In its simplest form HELIOS is a large cavity, or pressure vessel, filled with high-temperature and pressure gas. This gas is obtained by introducing it cold to the chamber and then adding a large amount of energy. A plug in the throat of a nozzle attached to the vessel is removed and the gas flows out the nozzle, producing thrust.

What we feel is reasonable to include on the rocket for which HELIOS is the engine is shown in Figure 1, which may or may not bear any relation to reality. Forward of the engine is shown a warehouse for the energy sources. Next are propellant tanks, biological compartments, re-entry vehicles, mission vehicles, and what-not. Since most of the thrust is produced by the nozzle, this has to be a fairly substantial structure. Shown in Figure 1 are superstructures surrounding the nozzle which would be dead, wasted weight to be carried along.

Figure 2 is a rather exotic device by which we bring this dead weight back to life. We use the nozzle itself as part of the structure. The biological compartments, mission vehicles, and propellant storage tanks are carried on the edge of the nozzle. The skirt on the end of the nozzle was placed there by the artist to serve as a warehouse for the nuclear devices. The nozzle expansion ratios we talk of are on the order of 100 in area.

In all of the schemes that have been discussed so far in the meeting, there are two questions that must be answered. First, is it possible to build the machine, and the second, is it worth building? I believe that we can categorically state that it is possible to build this engine given enough mass. Naturally, our primary concern is seeing just how light we can build the engine--and still make it work.

[redacted]

[redacted]

As was mentioned, the idea has been discarded several times previously. The reasons for this were two-fold. First, until recently, reliable steels had yield strengths below 100,000 psi, and second, nuclear device technology dictated that reproducible yields were in excess of 20 tons of H.E. equivalent energy, and that in order to make efficient use of the nuclear fuel the yields had to be in the kiloton range.

How these two figures tend to fix the weight of the pressure vessel is explained as follows. If we assume that the nuclear energy is transformed into the internal energy of a perfect, γ-law gas contained within an elastic, thin-shelled, spherical container, then it is quite simple to show that the total weight of the pressure vessel is a linear function only of the specific internal energy of the gas. A few years ago it was estimated that the constant of proportionality between shell weight and nuclear yield was 100 tons of pressure shell per ton of yield. This, coupled with a minimum of 20 tons of yield, indicated excessive engine weights. Recent advances in materials technology have led us to believe that a value of 20 tons/ton is realizable. This will be discussed in a bit more detail later. Additionally it is felt that it is not unreasonable to consider nuclear yields down to around 2 tons of H.E. equivalent.

Soon after the energy of the nuclear device is released the vessel will be subjected to nuclear radiation, recurrent shock waves, high pressures, thermal radiation, and energy transfer by conduction and convection from high temperature gas. In order to arrive at quantitative estimates of the internal environment of the shell, we ran a series of problems on one of the existing digital computer codes at LRL. The code used was designed for the weapons program, and the equations-of-state are known to be incorrect in our region of interest, although not grossly so. The greatest inaccuracy is in the computation of radiation transport. However, we expect that the results are not grossly in disagreement with nature.

Figure 3 shows the computed pressure on the inside of the vessel wall as a function of time. The first spike is the initial shock wave that hits the wall and reflects back inwards to the center of the cavity and reverberates repeatedly between the wall and the center. There may well be structural problems created by the shock waves traveling through the material of the pressure vessel. We are just beginning an experimental program to determine the internal behavior of metals under repeated, low-intensity shocks. Figure 4 indicates the response of the shell to this sort of a pressure history. The wave labeled "b" represents response of the shell to a step in pressure to the final steady-state pressure. The curve labeled "a" is the response of the shell to the same pressure step with a short, square-wave

[redacted]

pulse near time t = 0. We have shown that the pressure profile of the previous slide yields about this same response with minor corrections for the later reverberations.

We expect the pressure in the vessel to start dropping noticeably in a few milliseconds. From Figure 3 we see that the gas is not too far from hydrodynamic equilibrium at times of this order. This exhaust-time scale is varied by the area of the exhaust port. At present the nozzle throat is fixed such that about 90% of the gas will be exhausted in around a tenth of a second. From Figure 4 we see that there is an overshoot of the wall displacement from what would be expected from a step in the pressure. It is something like two and a half times the mean pressure expansion. The weight/yield constant of 20 tons/ton quoted earlier comes from increasing the weight of the pressure shell by a factor of four over that which would just contain the steady-state pressure without yielding. This slide indicates that we only need a factor of 2.5; however, this would leave no safety margin. The factor of four is used throughout all of our performance and mission analyses.

Perhaps our most serious and least understood problem is the energy transfer from the gas to the vessel. Very crude calculations indicate that there will be something like 100 cal/cm^2 deposited on the inside of the wall of the pressure vessel. About 10% of this comes from the initial fire ball, and will be deposited within the first milliseconds. We need very much to have a physical understanding of the processes that go on here. We are working on this from a purely theoretical standpoint at the moment. The high-energy deposition rate from the fireball may necessitate the use of some kind of ablative coating on the inside of the wall.

At any rate, we believe that there will be between 3 and 4% of the total nuclear energy, of the total energy released, deposited in the metal itself. Perhaps half a percent of this will be in the form of dynamic ringing of the vessel.

This 3 to 4% of the energy that gets into the wall will account for something like a 15 to 20°K rise in the temperature of the wall per pulse. Sooner or later, it will be necessary to remove the heat from the wall as demonstrated in Figure 5. Here is plotted the effective strength as a function of temperature and pressure. The q is that "safety" factor four; omega is the tons/ton of yield which, it will be remembered, was claimed to be completely constant, dependent only on the energy contained within the pressure vessel. This is true only for a perfect γ-law gas which hydrogen is not, at temperatures in the dissociation region. The formula for omega includes a factor which is the ratio of the PV energy of the gas to its internal

energy. The fact that this ratio is a complicated function of both P and E generates the three different curves shown. From Figure 5 we see that the weight of the pressure shell needed to contain this energy is fairly flat as a function of temperature up to around 700°K, then it starts rising rapidly. In order to keep the weight to a minimum, we must keep the temperature as low as possible. Since energy cannot be radiated to space from a body at 700°K rapidly enough to be commensurate with the pulse rates we contemplate, it seems that the only reasonable place to deposit this energy is in the propellant itself. Even there, energy may not be removed from the wall unless there is a temperature difference maintained between the propellant and the wall. It will take several pulses to get up to a reasonable temperature difference, and we feel that we can maintain this difference by propellant flowing through the pressure shell wall. Naturally, if we were to expel the gas faster, we wouldn't have as much of a heating problem; but this would say that there would be more peak thrust from the engine which would demand that the nozzle and shock absorbers be increased in strength and weight. There would thus appear to be some optimum peak thrust dictated by the cooling requirements of the pressure shell and the mass requirements of the nozzle.

As the gas expands out the pressure vessel, it follows the curve given in Figure 6, if an infinite nozzle, complete recombination, and 100% isentropic efficiency are assumed. We have performed some hand calculations to determine the effect of a fixed expansion ratio nozzle. We found that this actually tends to sharpen up the shoulder of the curve. Naturally, it drops the whole I_{sp} curve; but the I_{sp} does hold up flatter a little longer before it starts dropping off. We must also include the effects of recombination and the effects of a fixed amount of contaminant from the energy source, perhaps 70 lb, in the propellant. This also has to be included in the hydrodynamic calculations. We must know what effect the contaminants have on the recombination rate. We suspect that it will increase the rate by catalysis. This is something that we have not done much work on and will have to look into.

The basic question in our minds is the value of building the engine--as it seems possible to do so. The answer to this entails a certain amount of mission analysis. Very preliminary, but indicative results are given in Figure 7. It has been stated that mission analyses are to be avoided for this conference; however, we feel that they are necessary for an understanding of the problems of HELIOS.

We have assumed for this a payload of 50 tons. The equilibrium temperature of the gas would be 6000°K and the pressure 100 atmospheres.

[redacted]

We have assumed a rather optimistic Martian mission ΔV of 60,000 feet/sec for our analysis.

Included in the analysis are analytic, dissociating-gas, thermodynamic properties for hydrogen, the rocket equation, material properties of steel for the pressure shell, and fairly optimistic estimates of tankage and nozzle weight. The thin-shell approximation was used to obtain the vessel radius and mass. Exclusive of specific impulse, the quantities obtained from this analysis are, in part, listed in Figure 7. It turns out that there are three independent variables which must be specified to completely determine a given system; and these we chose to be temperature, pressure, and specific impulse. One might wonder how specific impulse could be an independent variable here. This obtains because we fix the amount of energy-source debris we have in the propellant at 70 lb. The rest of the gas is hydrogen. The debris is treated as a perfect, $\gamma = 5/3$ gas of molecular weight 12. Figure 7 is a typical page of computer output and shows, for example, that if we want 1800 sec specific impulse from the given conditions, the mass fraction of hydrogen would then have to be 96%. Now with 70 lb of debris, the mass of gas in the cavity is quite large. The vessel radius would be something like 30 ft and the yield around 40 tons, which means that the pressure vessel would have to be quite heavy. The number of pulses for this particular case is around 2000. This is a fairly low number, because of the high specific impulse and the large amount of propellant exhausted per pulse. The total mass of the rocket is quite large because of the large engine weight.

Now at the other extreme in I_{sp} we see that we need only a small yield and a low weight percentage of hydrogen in the bottle. However, the low mass expelled per pulse and low I_{sp} demands many such pulses for a given mission ΔV. In this case a large total rocket mass is produced from the rocket equation with low I_{sp} rather than a high engine weight, as in the high I_{sp} case. As shown, between these extremes there is a minimum in total weight.

We have devised a figure-of-merit for a given set of parameters which we guardedly call the mission cost. It is expected that the amount of fissionable fuel is around 1 kg per pulse. We take \$50,000 to be the cost per pulse. NASA indicates that \$200 per pound is not an unreasonable freight charge to place the total mass in orbit. Our figure-of-merit is the sum of these two. We find that the minimum in mission cost occurs not too far from the minimum in total mass. Thus, for these particular parameters the least expensive mission would start with around 700 tons in orbit, have average I_{sp} a bit above 1500 sec, and use between 4000 and 5000 pulses.

Question: And the I_{sp} is at equilibrium?

[redacted]

Answer: It is the equilibrium value multiplied by some number less than one to account for the effects of a finite nozzle, finite recombination, and pulsing. We have used 0.8 for the results given in Figure 7.

Answer (Cooper): The point is that if the energy of the bomb were added to pure hydrogen, the temperature would be over 10,000°K. However, the energy is divided between the hydrogen and the bomb material which has a molecular weight of 10 or 12. This extra material thus lowers the temperature and raises the average molecular weight resulting in a lower equilibrium specific impulse

One good feature of this machine is that it can be tested underground. In this connection one can conceive of many good physics experiments that can be carried out with a pressure vessel which could contain a nuclear shot.

Question: What is the time between shots?

Answer: There is no a priori fixed time between pulses. This depends upon the cooling rate of the vessel and the complexity of introducing the next device. We want to make the pulse rate as fast as possible. Typically, in the absence of shock absorbers, the acceleration is about a 2 g pulse lasting for a tenth of a second. Now, if you wait 10 sec between pulses the average thrust is then 0.02 g. We would like as high an average thrust as possible.

Question: Would you assume that your charges would need no shielding for radiation?

Answer: That's right. We have so far.

Question: Do you think this is realistic?

Answer: Perhaps not.

Question: You mentioned 1 kg of nuclear fuel. Is that a critical mass in this case?

Answer: Well, it depends upon how you build these devices. I can't go into that deeply, but I think 1 kg is about as low as you're going to go.

Answer (Cooper): I think that the point is, that it's kilogramish and that it's not 2 to 500 grams. A factor of two one way or the other is reasonable if the fuel is plutonium and somewhat larger, naturally, if you use uranium as the fuel.

Question: Does some of the propellant go through the wall? You can see that the dynamics of the shell would be changed when you have some flow of the coolant through the wall.

Answer: We have not yet considered the dynamic response of any structure other than a thin spherical shell. We would like, if possible, to spray the inside or have flow holes in the pressure vessel, which is going to increase the weight. Practically any modification of this sort is going to increase the weight of the pressure vessel. We should also be worried about the thermal stresses on the inside wall. This is something that we have not looked at closely and may well be one of the more serious problems.

Question: What do you think will be the total mission cost?

Answer: The last slide will give that to us.

Answer (Cooper): These are based on something like 50 tons round trip through 60,000 ft/sec, and the cost generally turns out to be divided about equally between the fuel and the weight that you have to put into orbit and the minimum cost is about the minimum weight. So, it's about $148,000,000 to put the thing into orbit, and it's something like a $140 to $200 million for the charges.

The total cost is thus around $500 million.

Question: How much hydrogen do you use per pulse?

Answer: Each case is different. Shown in this slide is the percent of hydrogen necessary to produce a given I_{sp}. As you will remember, we fix the weight of non-hydrogen additive at 70 lb. From this you can easily get the total mass of gas expelled per pulse. The numbers presented here are merely indicative of our general analysis.

Question: What's the average thrust to weight ratio for the engine alone?

Answer (Cooper): Well, he really answered the question before. It depends on the rate at which you fire; and in particular, it doesn't matter. I think they want to fire at such a rate that they have better than 0.1 g, on the average. We made some computations on ground take off, and then it appeared to be quite a problem. It was necessary to fire one per second or faster.

Answer: Well, if you wanted to take off, there are two problems. The first is a political one, and the second is how fast the engine can be pulsed.

Question: Was the mass number for the pressure shell based on the properties of maraging steel?

Answer: That's right. It's just about the best we can do. We don't know if the yield strength we assumed is an over or under estimate. We are just getting into the experimental study of the problem.

Answer (Cooper): Right. Oh, incidentally, let me mention that there's an unclassified report that Bob Fox[1] did on this, in I guess about 1957, which has almost all of this material.

1. R. H. Fox, "A Study of the Nuclear Gaseous Reactor Rocket," UCRL-4996, Oct. 31, 1957 (Uncl.)

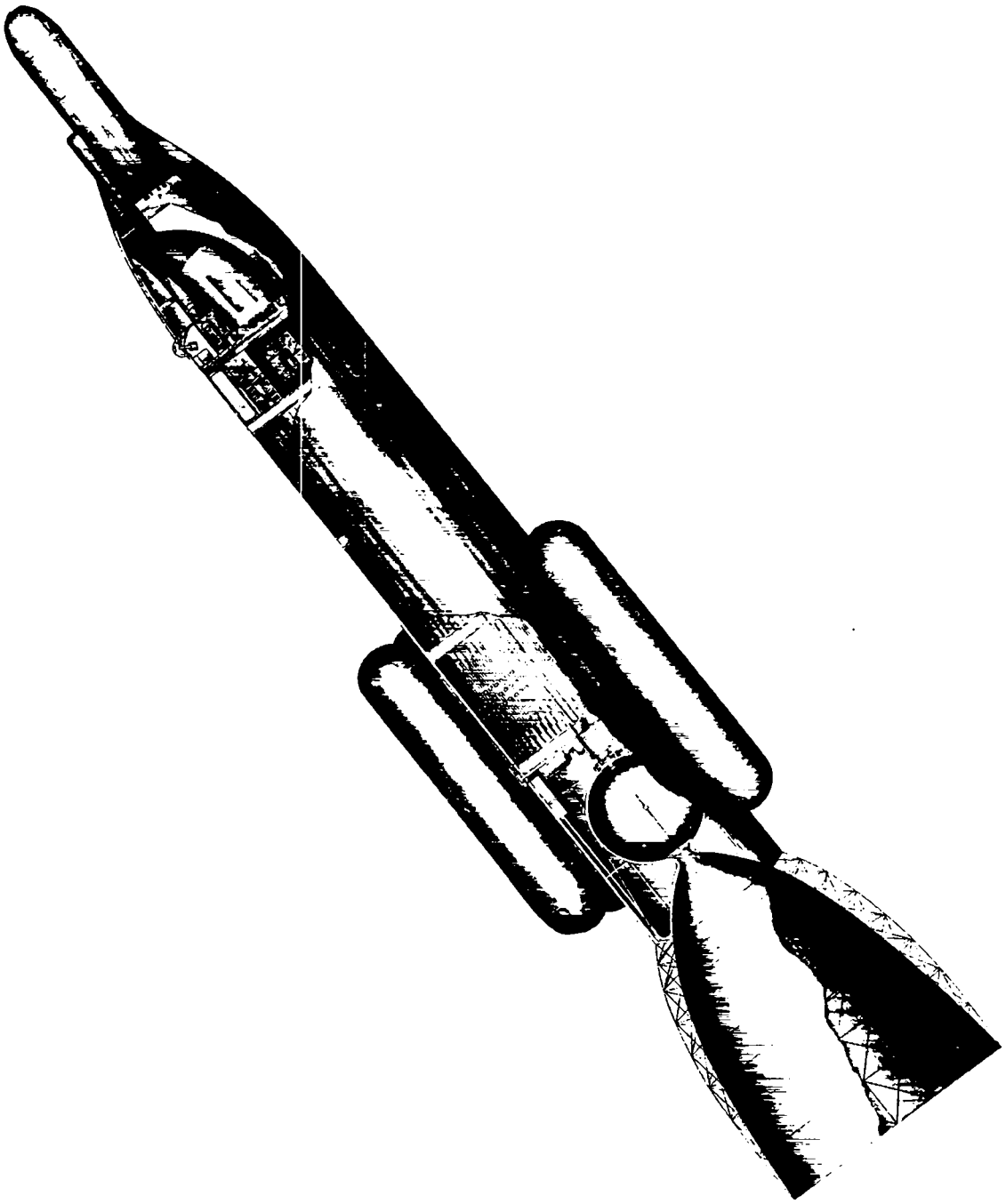

Figure 1

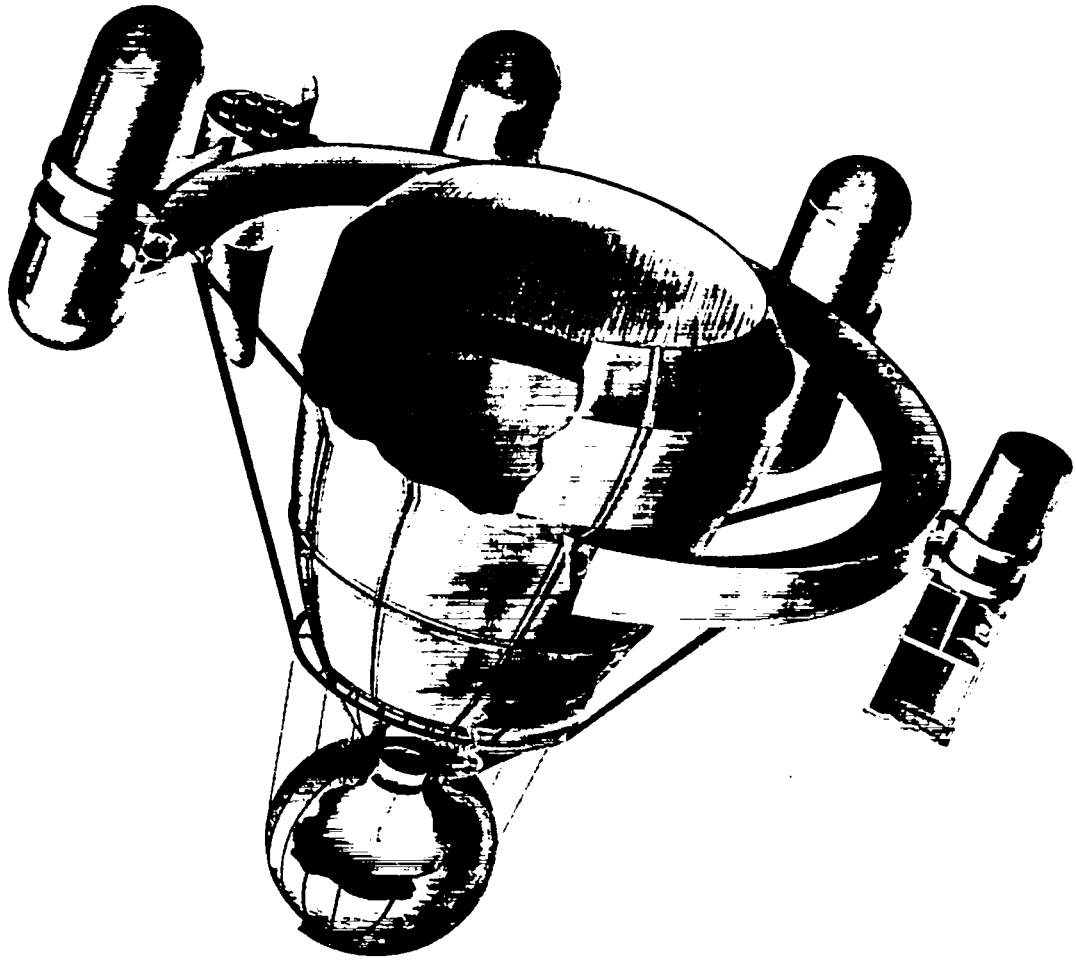

Figure 2

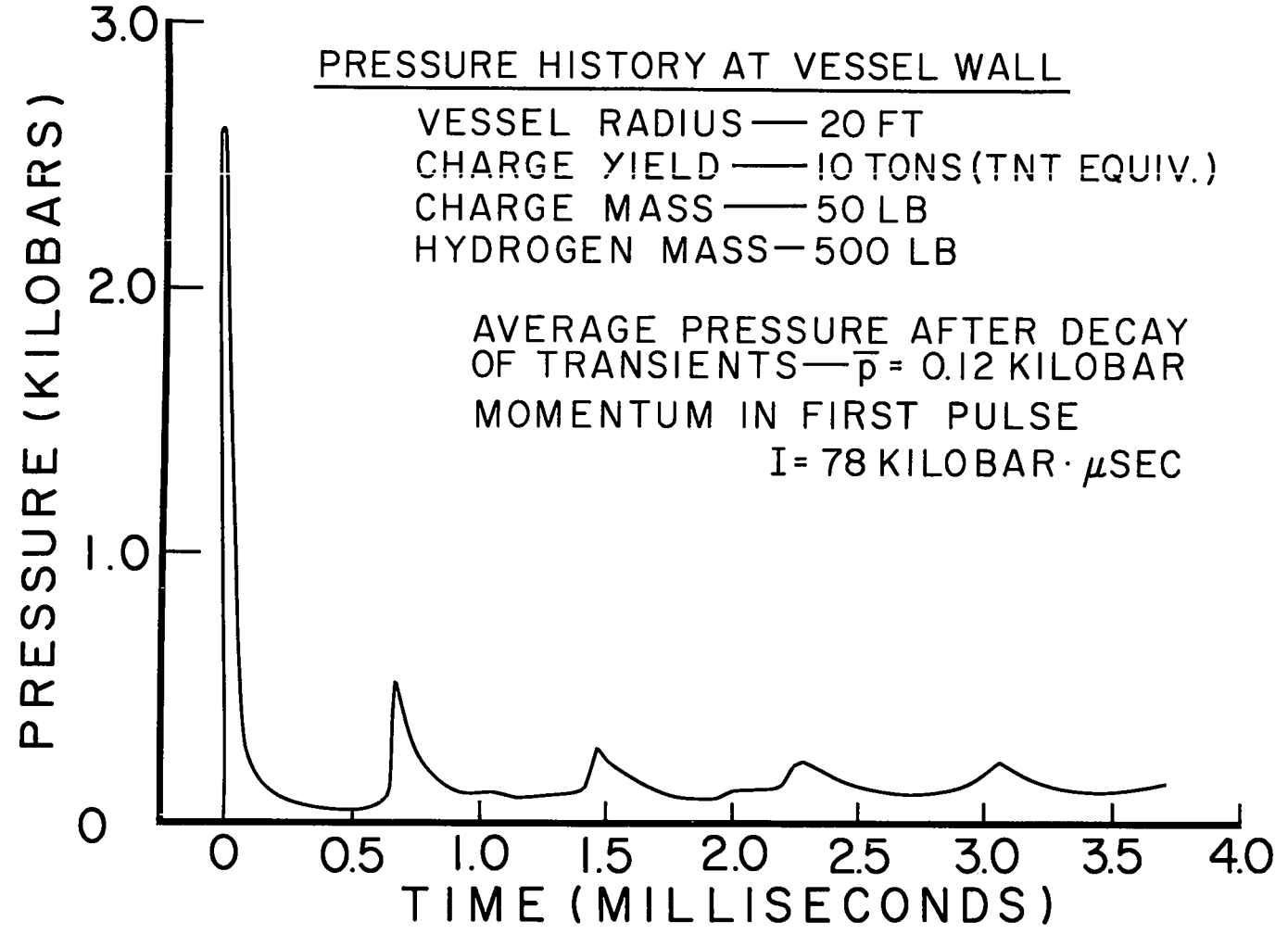

Figure 3

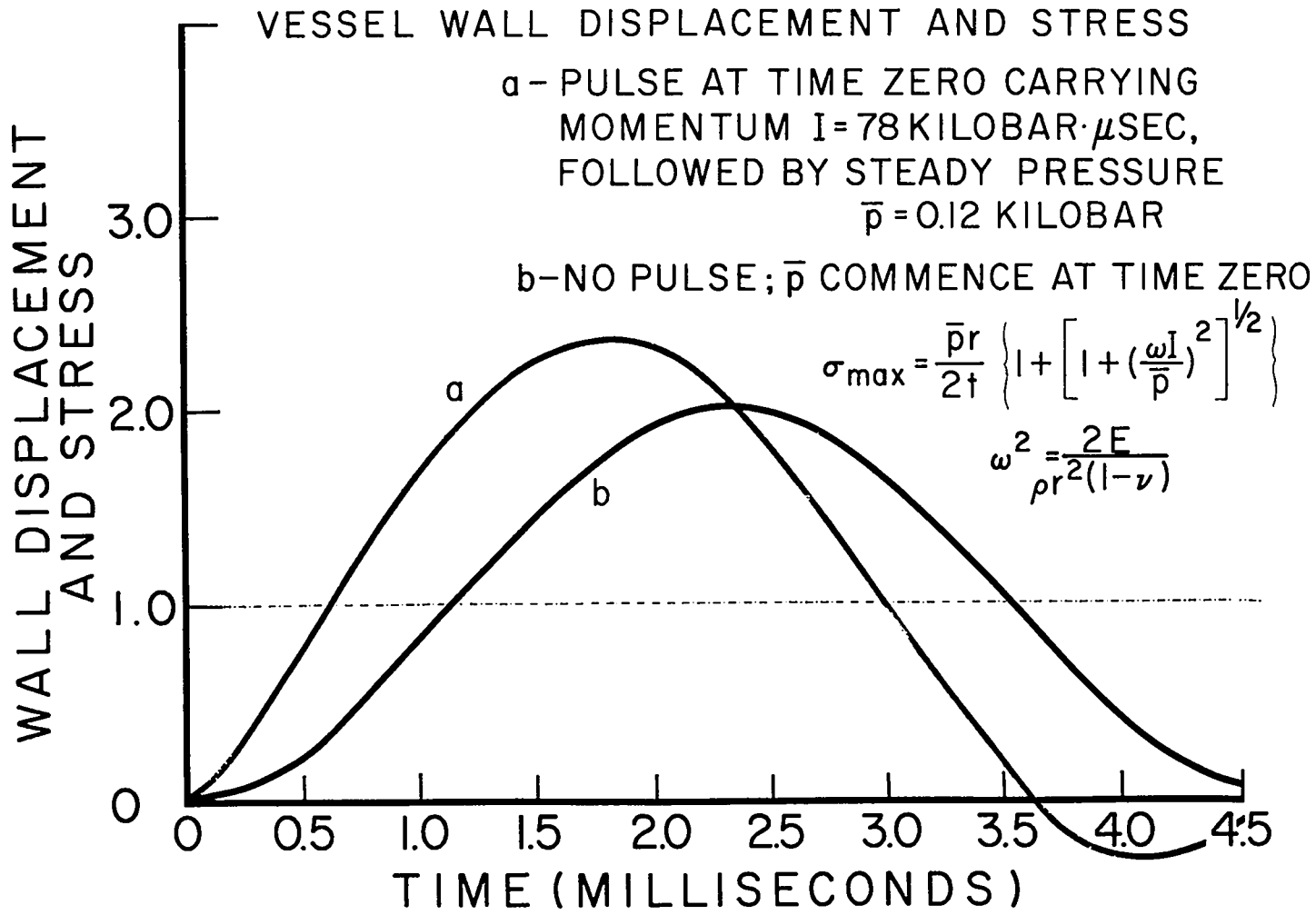

Figure 4

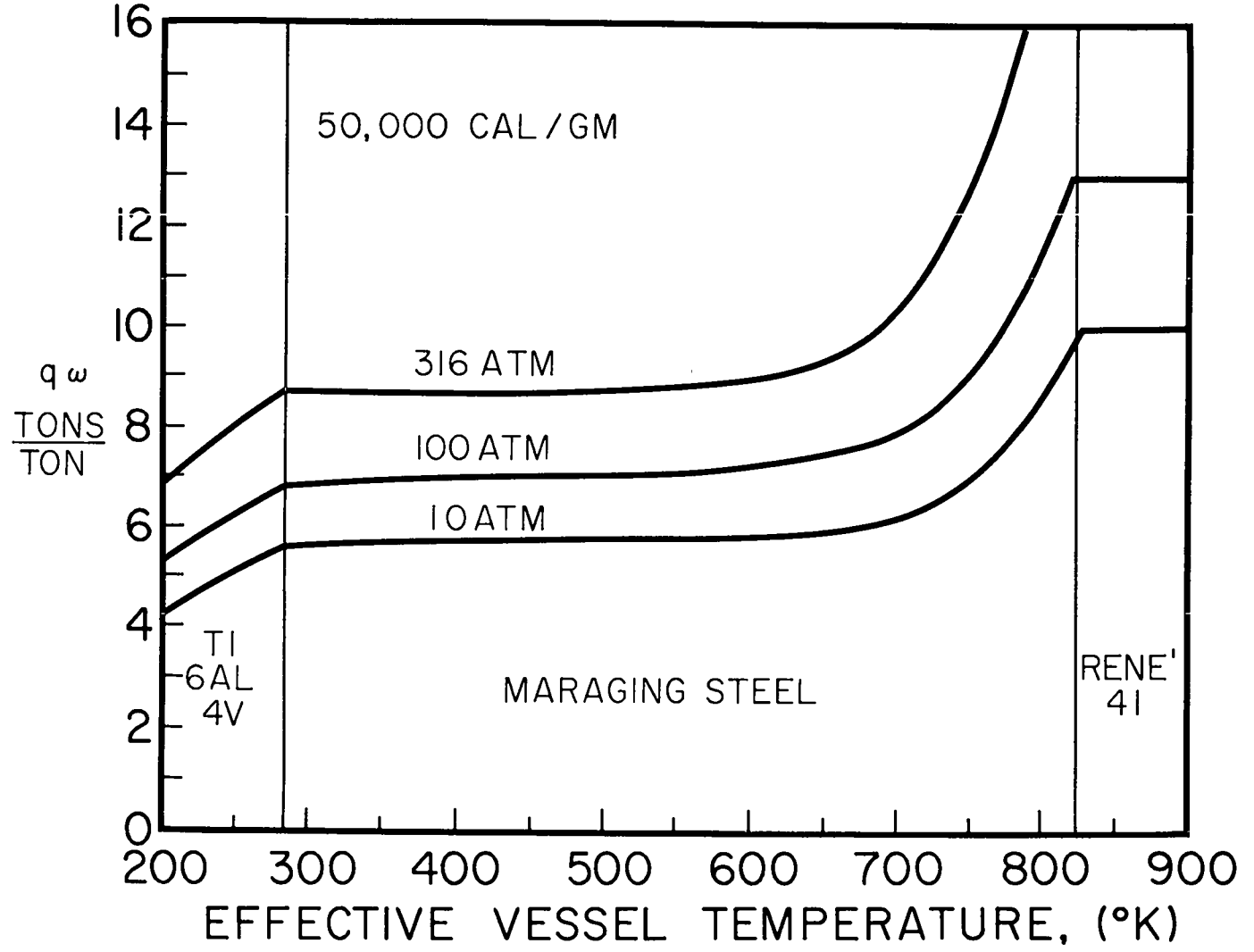

Figure 5

APPROVED FOR PUBLIC RELEASE

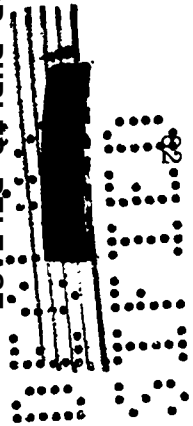

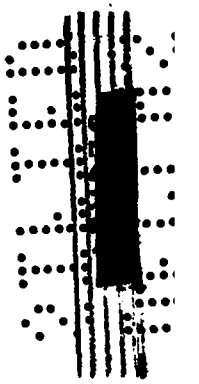

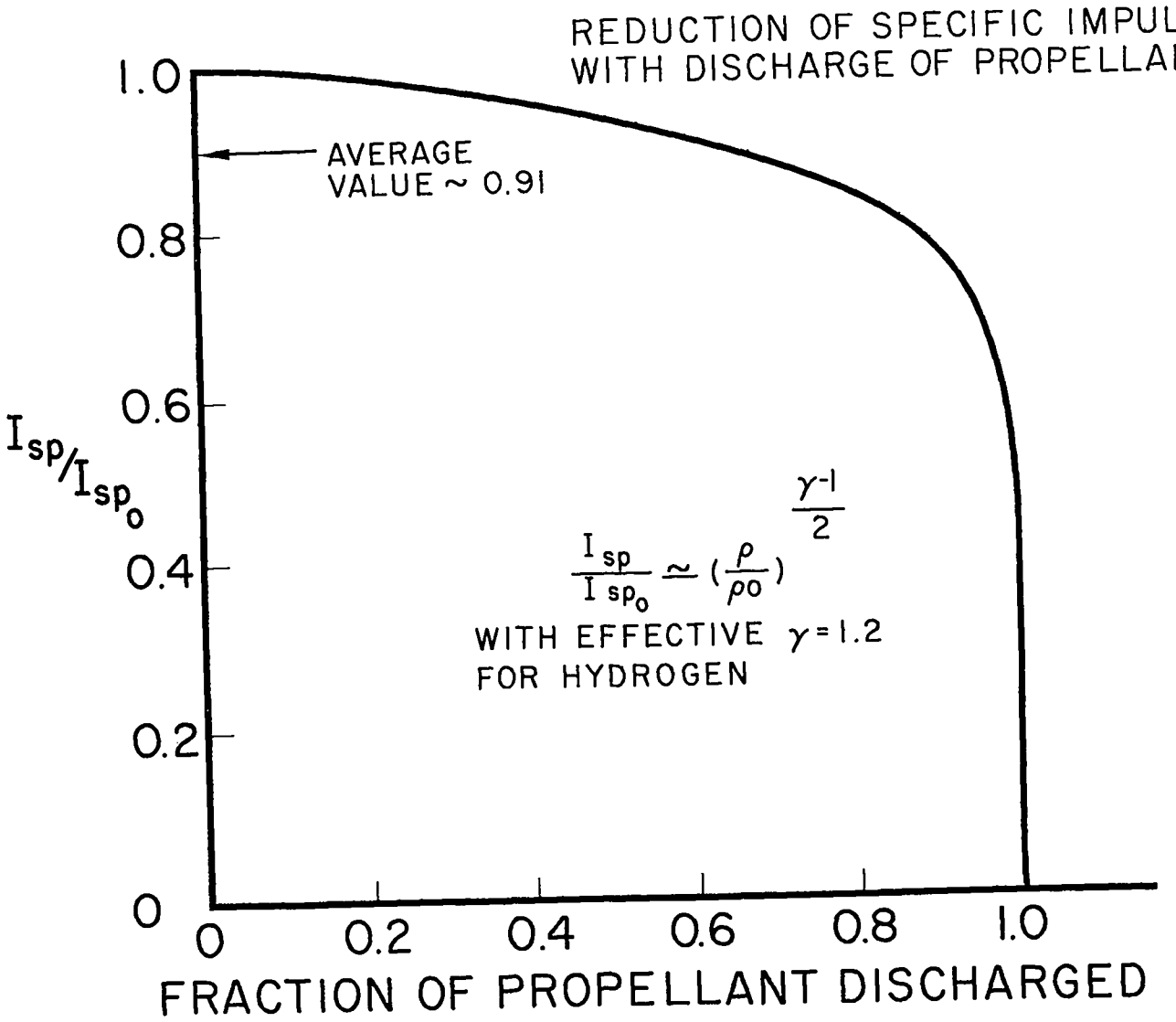

Figure 6

NUCLEAR PULSE ROCKET
TYPICAL PARAMETERS

PAYLOAD MASS ---------- 50 TONS

PROPELLANT — TEMPERATURE ---------- 6000 °K

PROPELLANT — PRESSURE ---------- 100 ATM.

IDEAL MISSION VELOCITY ---------- 60,000 FT/SEC

SPECIFIC IMPULSE	PROPELLANT % HYDROGEN	VESSEL RADIUS	CHARGE YIELD	NUMBER OF PULSES	TOTAL MASS
1800 SEC.	96	29.5 FT.	40.2 TONS	2108	2826 TONS
1740	89	20.7	14.1	2484	1227
1680	83	17.3	8.2	2934	877
1620	76	15.2	5.6	3482	757
1560	70	13.7	4.1	4166	707
1500	65	12.5	3.2	5042	701
1440	59	11.6	2.5	6208	730
1380	54	10.8	2.1	7836	798
1320	49	10.1	1.7	10,269	923

Figure 7

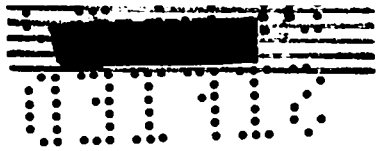

ORION

J. C. Nance and T. B. Taylor
General Atomic
San Diego, California

A copy of this presentation is not available as the edited transcript was not returned by the author. Referenced below, however, are two unclassified publications issued subsequent to the meeting; they give the fullest available presentations of subject matter on this topic except for classified nuclear explosive device design and effects information. They are:

1. Nance, J. C., "Nuclear Pulse Propulsion," IEEE Transactions on Nuclear Science, Vol. NS-12, No. 1, February 1965, pp. 177-182 (report of 11th Nuclear Science Symposium, October 28-30, 1964, Philadelphia, Pa., sponsored by the IEEE Group of Nuclear Science, the Atomic Energy Commission, and the Air Force Office of Scientific Research); also identified as GA-5572, 5 October 1964.

2. Shipps, Paul R., "Manned Planetary Exploration Capability Using Nuclear Pulse Propulsion," Proceedings of the Second Space Congress: New Dimensions in Space Technology, pp. 363-385 (April 5-7, 1965, Cocoa Beach, Fla., sponsored by the Canaveral Council of Technical Societies); also identified as GA-6224, 19 March 1965.